LEHRSTUHL FÜR EISEN- UND STAHLMETALLURGIE
MONTANUNIVERSITÄT LEOBEN

Evaluation of the potential for reduction of CO_2 emissions at the secondary metallurgy

Master thesis

eingereicht von

Andrey Gerasev, BSc

am Lehrstuhl für Eisen- und Stahlmetallurgie an der Montanuniversität Leoben
zur Erlangung des akademischen Grades

Diplomingenieur

in der Studienrichtung Eisen- und Stahlmetallurgie

MONTAN UNIVERSITÄT

Lehrstuhl für Eisen-und Stahlmetallurgie – Montanuniversität Leoben
Franz-Josef-Straße 18 – 8700 Leoben, Österreich

Acknowledgment

I would like to express my deep gratitude to supervisor, Dipl.-Ing. Philip Bundschuh. Without his continuous encouragement and support this study would hardly have been completed. He spent much time to instructing me how to collect data, develop the calculations and write this paper. Also I am grateful to Professor Schenk, who offered this interesting topic to me. Further he was always providing useful suggestions about this thesis. Both of these colleagues are high professional and I believe their academic achievements will continue to increase.

I would like to thank all the members from voestalpine Stahl Linz GmbH and RHI AG involved to this project. During our personal meetings and discussions we got many interesting ideas to develop this study. I consider as a honour to work with Ing. Andreas Viertauer, Dr. Bernhard Trummer, Dr. Roman Rössler and Dr. Peter Reisinger.

Last but not the least important, I owe my deepest gratitude to all my family, especially to my parents, for their support and encouragement through my life.

Abstract

Policies all over the world encourage the high energy efficiency of processes and the reduction of greenhouse gas (GHG) emissions, classified as direct and indirect ones. Iron and steelmaking is an energy-intensive industry, which also supplies 30% of the direct global CO_2 emissions (2007), triggered by the industrial processes. [1] This thesis focuses on the verification of the CO_2 emissions distribution for the secondary steelmaking, as well as in the evaluation of the potential to reduce such emissions.

The calculations of the current study are based on the ladle treatment for the recycling production route, comprising the transfer of crude steel from the electric arc furnace (EAF) via the ladle furnace (LF) to the continuous casting machine (CCM). The mass and heat balances for corresponding production route were calculated considering the steel- and slag chemistry. The alloying concept including the mass- and energy-balances was developed regarding to the basics of thermodynamic and industrial operation practice.

The main influences for the variation of the CO_2 emissions contribution in the ladle metallurgy are the additions during tapping, logistics of the ladle and ladle preheating treatment. These three influences were set as the most important for the following estimation of the potential savings and reduction of CO_2 emissions. Estimation of the emission distribution and evaluation of the saving potential were analysed due to the different logistic- and configuration -assumptions. The potential for savings were also recalculated in terms of electricity consumption for the LF-treatment.

Kurzfassung

Der Grundsatz energieeffizienter Produktionsverfahren wird auf der ganzen Welt forciert, um eine Reduktion von Treibhausgasemissionen (THG), die als direkte und indirekte eingestuft werden, zu erreichen. Die Eisen- und Stahlerzeugung ist eine energieintensive Industrie, die 30% der direkten globalen, industriellen CO_2 Emissionen (2007) verursacht. Diese Arbeit konzentriert sich auf die Erfassung der Verteilung der CO_2 Emissionen für die Sekundärmetallurgie sowie auf die Bewertung möglicher Einsparungsmaßnahmen.

Die Berechnungen der aktuellen Studie wurden für die Rohstahlbehandlung in der Pfanne, während der Überführung des flüssigen Stahls aus dem Elektrolichtbogenofen (ELBO) zur Stranggießanlage (CC), durchgeführt. Die Rohstahlbehandlung umfasst die Prozesse des Stahllegierens und des Stahlheizens, nach den Stahlgüteanforderungen. Weiters, wurden unter Berücksichtigung der Stahl- und Schlackenchemie, die Massen- und Wärmebilanzen für die jeweiligen Produktionsverfahren berechnet. Das Legierungskonzept und die Stoff- und Energiebilanzen wurden auf den Grundlagen der Thermodynamik und der bewährten industriellen Betriebspraxis entwickelt.

Der Legierungsmix beim Abstich, die Transferzeit der Pfanne und die Vorheizdauer der Pfanne, wurden als die wichtigsten Parameter für die folgende Abschätzung der möglichen Energieeinsparungen und die Reduzierung von CO_2 Emissionen festgelegt. Durch Variation dieser Parameter gelangen eine Einschätzung der Emissionsarten und eine Beurteilung der potentiellen Einsparungsmöglichkeiten von Treibhausgasen. Außerdem konnten Möglichkeiten zur Energieeinsparung gefunden werden.

Affidavit

"I confirm that I wrote this thesis independently and on my own without using any other sources and aids as I stated. Where I used other sources I clearly marked them as not my own. This thesis has not been received by any examination board, neither in this nor in any similar form. Furthermore, I agree to an anonymous test of plagiarism which electronically verifies the validity of my declarations. I am aware that my thesis will not be evaluated in case of not making this statement."

.....

Andrey Gerasev

Table of contents

General formula symbols

{ }	Gas phase
[ ]	Melt
( )	Slag phase
<>	Refractory material, nonmetallic inclusions

Acronyms

β	Expansion coefficient
ε_{shell}	Emissivity coefficient of the steel shell
ε_{slag}	Emissivity coefficient of the slag
λ	Heat conductivity
ν	Viscosity
σ	The Stefan–Boltzmann constant
a	Coefficient of thermal diffusion
a_o	Activity of oxygen
Al_2O_3	Aluminium oxide
$[Al]$	Target value of aluminium in steel after completed alloying
ALL TAP	Alloying by tapping
ALL LF	Alloying in ladle furnace
B_2	Basicity ratio
B_4	Basicity ratio
BAT	Best available technology
BF	Blast furnace
BOF	Basic oxygen furnace
CaO	Calcium oxide

$CaMg(CO_3)_2$	Dolomite stone
CO	Carbon monoxide
CO_2	Carbon dioxide
CH_4	Methane
c_p	Isobar heat capacity
$c_{p\ i\ liquid}$	Heat capacity of melted addition
$c_{p\ \ i\ 298}$	Heat capacity in solid condition
CAST	Casting on Countinious Casting Machine
CCM	Continuous casting machine
$dH_{CO_2}^{carb.}$	Enthalpies of decomposition
$dH_{i\ oxidation}$	Enthalpy of the oxidation for the metal phase component i
DL-A1	Assumption for concept with doloma, “good logistic” and no cover
DL-A2	Assumption for concept with doloma, “good logistic” and cover
DL-B1	Assumption for concept with doloma, “bad logistic” and no cover
DL-B2	Assumption for concept with doloma, “bad logistic” and cover
DL-concept	Alloying concept with doloma
DRI	Direct-reduced iron
EAF	Electric arc furnace
EJ	Exajoule
g	Oxide to generate
g	Gravitational acceleration
GHG	Greenhouse gases
GJ	Gigajoule
Gt CO_2 yr	Gigatonnes of carbon dioxide per year
GWP	Global Warming Potential
$H_{crude\ steel}$	Amount of heat of the steel before alloying

$HG_{oxidation}$	Amount of heat generated due to oxidation
H_{298}	Enthalpy of the element in its stable condition (298K)
ΔH_{Tr}	Enthalpy for the phase transformation
$HL_{decomposition}$	Amount of heat lost due to decomposition
$HL_{sensitive}$	Amount of sensitive heat losses
$H_{latent\ melting}$	Amount of latent heat
$HL_{sensitive}$	Amount of latent heat losses
$H_{alloyed\ steel}$	Amount of heat in steel after alloying
$H_{crude\ steel}$	Amount of heat in steel before alloying
$HL_{per\ heat}$	Amount of heat losses due to the ladle's configuration per one heat
i	Chemical element
IEA	International Energy Agency
IPCC	Intergovernmental Panel on Climate Change
IR	Integrated route
j	Alloying agent
j	Slag former
J	Joule
kg/t_{ls}	Kilogram per ton of liquid steel
kJ/s	Kilojoules per second
kW	Kilowatts
kWh/t_{ls}	Kilowatts per t_{ls}
kg_{CO2}/t_{ls}	Kilogramm of carbon dioxide per t_{ls}
l	Thickness of the layer
LF	Ladle Furnace
Mod.	Module
$m_{alloyed}$	Alloyed mass

$m_{alloying\ (i)}$	Alloying mass of chemical element
Mt	Megatonnes
MgO	Magnesium oxide
$MgCO_3$	Magnesium carbonate
$m_{alloyed\ (i)}$	Alloyed mass of chemical element
$m_{before\ alloying\ (i)}$	Mass of chemical element before alloying
$m_{after\ alloying\ (i)}$	Mass of chemical element after alloying
$m_{EAF-steel}$	Mass of steel before alloying
m	Metal
$m_{(o)in\ slag}$	Mass of oxide in slag
$m_{alloying_{(o)}}$	Mass of oxide, contained in the added slag formers
$m_{oxidated_{(o)}}$	Mass of oxide, generated via oxidation during alloying
M_o	Molar mass of oxide
M_m	Molar mass of metal
M_r	Molar mass of oxide to reduce
M_g	Molar mass of oxide to generate
$m_{alloying_{(c)}}$	Alloying mass of carbon
M_{CO_2} , M_C	Molar masses of carbon dioxide and carbon
m_i	Mass of corresponding alloying agent
$m_{crude\ steel}$	Heat size
$m_{carbonate}^{CO_2}$	Mass of CO_2 in carbonate
MJ	Megajoule
N_2O	Nitrous oxide
N_u	Nusselt number
o	Oxide in slag
$[O]_{alloying\ by\ tapping}$	Target value of oxygen in steel after alloying by tapping

$[O]_{alloying\ in\ LF}$	Target value of oxygen in steel after alloying in ladle furnace
(P_i)	Partial pressure
ppm	Parts per million
Pr	Prandtl number
PURG	Purging during LF-treatment
$Q_{conductivity}$	Heat flow conductivity
$Q_{convection}$	Heat flow convection
$Q_{radiation}$	Heat flow radiation
Q_{loss}	Amount of heat to purchase during LF-treatment
r	Oxide to reduce
$r.\%$	Recovery rate
$r.\%_{(c)}$	Recovery rate of carbon during alloying by tapping
Ra	Rayleigh number
RM-A1	Assumption for concept with raw magnesite, “good logistic” and no cover
RM-A2	Assumption for concept with raw magnesite, “good logistic” and cover
RM-B1	Assumption for concept with raw magnesite, “bad logistic” and no cover
RM-B2	Assumption for concept with raw magnesite, “bad logistic” and cover
RM-concept	Alloying concept with raw magnesite
RR	Recycling route
S	Area of the conductive surface
S_{mirror}	Area of the slag mirror surface
SINTEF	The Foundation for Scientific and Industrial Research
SiO_2	Silicon dioxide
$special\ Q_{loss}$	Amount of heat to purchase during LF-treatment per t_{ls}

tCO_2/year	Tonnes of carbon dioxide per year
$t_{heating}$	Duration of heating during LF-treatment
$t_{LF-Treatment}$	Duration of LF-treatment
$T_{cover\ inside}$	Temperature of inside surface of cover
$T_{cover\ outside}$	Temperature of outside surface of cover
$T_{steel-tapping}$	Tapping temperature of steel
$T_{side\ wall}$	Temperature of side wall
$T_{to\ compensate}$	Steel temperature to compensate during LF-treatment
TL_{Cast}	Temperature losses during casting
TL_{total}	Temperature losses due to the ladle's configuration total
TL_{Tap}	Temperature losses during tapping
$TL_{LF-Treatment}$	Temperature losses during LF-treatment
TAP	Tapping
TMC	Technometal Converter
TSTL	Total steel temperature losses
ULCOS	Ultra-Low Carbon Dioxide Steelmaking
VD	Vacuum Degassing
VOD	Vacuum Oxygen Decarburization
VODC	Vacuum Oxygen Decarburization Converter
$w.\%_{(i)}$	Weight content of chemical element
$w.\%_{(CO_2)}\ i$	Weight content of carbon dioxide in alloying agent
WT1	Waiting time after EAF tapping and before start of LF-treatment
WT2	Waiting time after LF-treatment finished and casting started
WT3	Waiting time after casting
°C	Celsius degree

List of figures

List of tables

1 Introduction

Our planet is facing a lot of man-made damage. The climate change is recognized as one of the most critical challenges ever to face humankind. The United Nations Framework Convention on Climate Change sharing the objective to stabilize atmospheric concentrations of greenhouse gases – enable such a global response to climate change. [2]

A greenhouse gas (GHG) is any gas in the atmosphere which absorbs and re-emits heat, and thereby keeps the planet's atmosphere warmer than it otherwise would be. The greenhouse gases occur naturally in the earth's atmosphere, but such human activities like the burning of fossil fuels are increasing the levels in the atmosphere. The most common GHGs in the Earth's atmosphere are water vapour, carbon dioxide (CO_2), methane (CH_4) and nitrous oxide (N_2O). The Kyoto Protocol is an international treaty for controlling the release of GHGs from human activities. Based on this protocol, Intergovernmental Panel on Climate Change (IPCC) formed a term "GWP" - Global Warming Potential. This potential is modified by different lifetime of gases in the atmosphere and the different heat absorbing capacity. Carbon dioxide has the "GWP"-index value 1. Other greenhouse gases are associated with bigger values. For example, 1 kg of methane causes 25 times more warming over a 100 year period compared to 1 kg of CO_2, that GWP value of CH_4 is 25. But still, carbon dioxide is considered as the most important GHG in terms of the quantity globally released and the total impact on global warming and the climate change. [3,4]

At the present time global direct GHG-emissions are rising and the largest growth in last decade has come from the power generation and industry sectors. The global primary energy use almost doubled from 225 EJ in 1970 to 470 EJ in 2004. It has a significant effect on the growth of energy-related CO_2 emissions, because about 70% of today's global energy

is supplied by fossil fuels. Nearly one-third of world's energy consumption is attributable to manufacturing industries. [1,5]

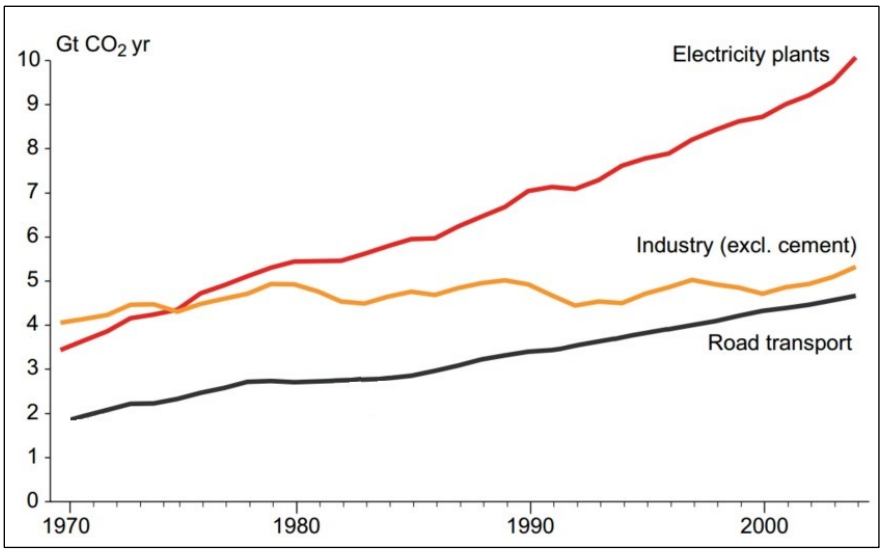

Figure 1-1: Sources of global direct CO_2 emissions, 1970-2004 (only direct emissions by sector) [5]

In general, the verifying of CO_2 emissions by industrial sector requires determination of direct and indirect emissions. Direct emissions are controlled by production and indirect are owned. Furthermore, all GHG emissions associated with all the industrial processes can be divided into three *Scopes*. *Scope 1* includes only direct emissions that are produced during industrial operations, for example fuel combustion. *Scope 3* are all indirect emissions from the entities operations, except the consumption of purchased electricity, which are classified as *Scope 2.* [6]

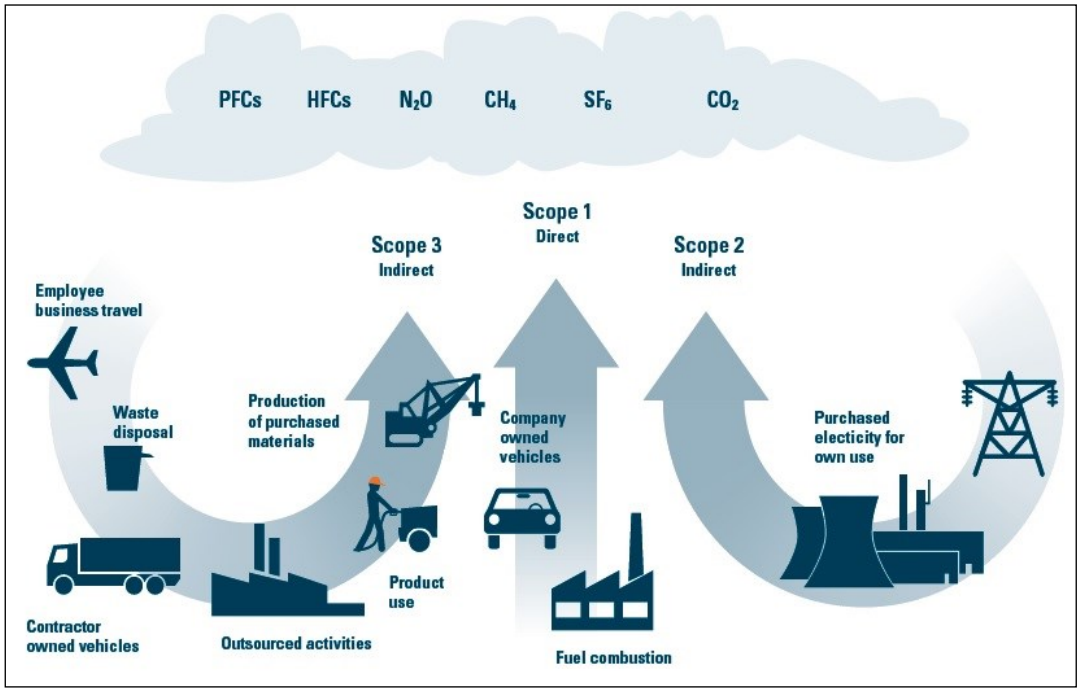

Figure 1-2: Greenhouse gas emissions, associated with industrial processes [6]

In 2007, total global direct CO_2 emissions from industry were 7.6 Gt of CO_2. The indirect emissions are associated with 4.3 Gt of global industrial CO_2 emissions. The largest contributors of direct CO_2 emissions by the industrial sector are iron steel and cement production. These industries collectively contributed 56% of direct emissions in 2007. With item "other" on the **Figure 1-3** is mentioned smaller processes like manufacturing of textiles, machinery and equipment. [1,7]

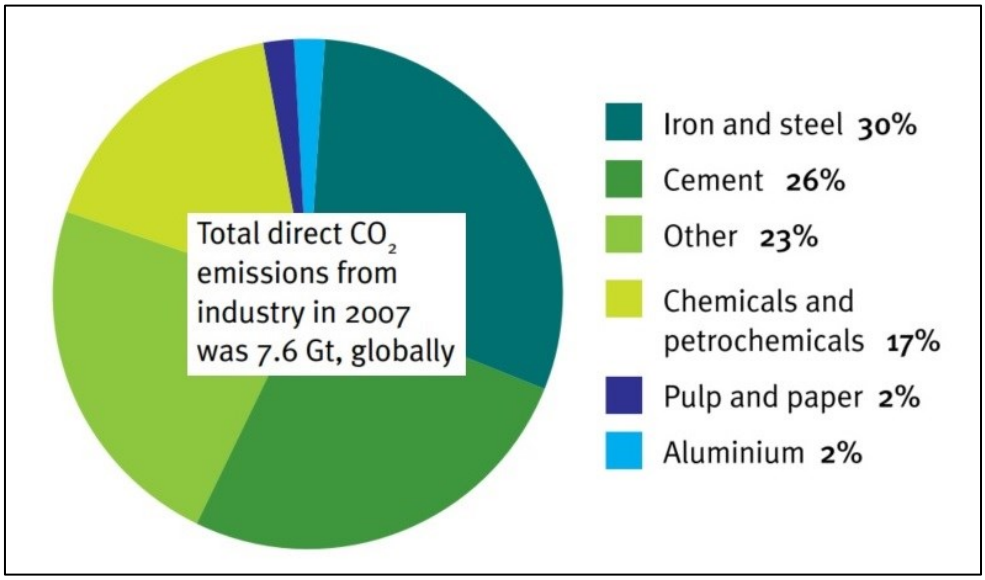

Figure 1-3: Global share of direct CO_2 emission by industry sector [1,7]

In the last decade, the steel industry achieved a great progress to reduce its energy consumption and its environmental impact. In the last 30 years annual steel production grew 93%, while its energy use rose only by 30% and its CO_2 emission impact increased only by 17%. These rates are explained by the raised use of recycled materials in steelmaking industry. The total scrap recovery significantly increased in last decade from about 325 Mt to 450 Mt. Even through the recycling rate is high, an expanding economy has meant that the total crude steel production is roughly twice the amount of scrap collected and used. So, the scrap availability is the main limiting factor here. [8]

1.1 CO_2 emissions in the steelmaking industry

In general, there are two main routes to produce the steel. The integrated route (IR) – used for 70% of production globally - is based on the steel production from iron ore. Today most of the CO_2 generated by steel industry comes from the chemical interaction between carbon and iron ore in blast furnaces used by this production route (**Figure 1-4**). The iron reduction process operates close to the thermodynamic limits. Best available techniques (BAT) for the BF-BOF route have energy efficiency around 20 GJ / ton hot rolled product (**Figure 1-4**). [9]

About 29% of steel is produced via recycling route (RR), where the scrap is used as the main raw material in electric arc furnaces (EAF). The energy intensity of the RR is much lower - around 4.5 GJ / ton hot rolled product (**Figure 1-4**), but switching from IR to RR is limited by the supply of cheap electricity and steel scrap. Alternatives to these two routes include direct-reduced iron (DRI) technology and smelting reduction. On the one hand the advantage by these alternatives is that the raw materials do not need to be treated, but on the other hand, more primary fuels – natural gas for DRI and coal for smelting reduction - are required. Apart from that, Schenk concluded [10] that all three route are equal regarding energy consumption. Hence, a replacement of the blast furnace – converter route by gas-based direct reduction with a subsequent electric steelmaking with the target to reduce CO_2 emissions does not seem to be an economic solution. [9,10]

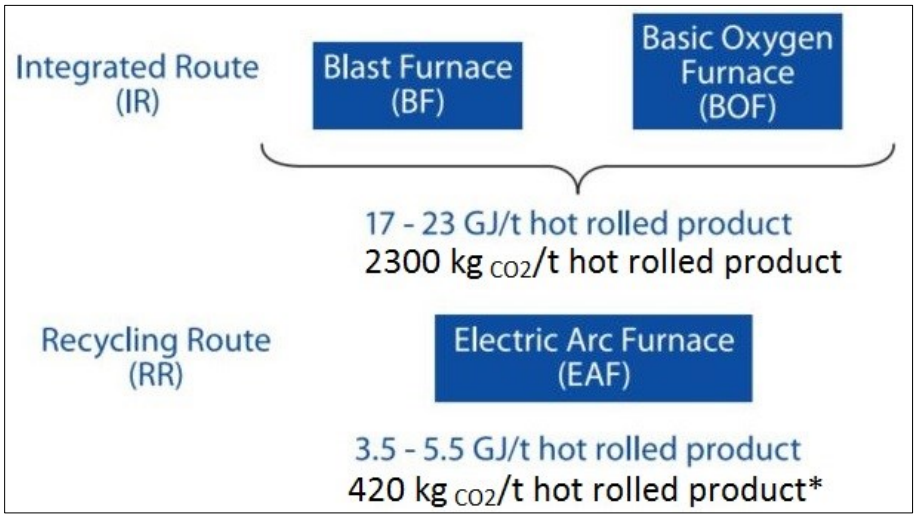

Figure 1-4: Energy efficiency and CO_2 emission for two main production routes in the iron and steel industry [9]

* Value is based on own calculation [11]

As was mentioned before (**Figure 1-2**), it is crucial to cluster the carbon dioxide emissions into direct and indirect, furthermore on three *scopes*. In terms of steelmaking and regulations from "Greenhouse Gas Calculation Tool" developed by World Resources Institute, this classification can be performed in a certain way. [6]

The *Scope 1*, associated with direct emissions, includes emissions that are produced directly during industrial operations. Basically direct emissions are caused by combustion processes. Also usage of different carbonates in steelmaking provides an extra amount of these emissions due to chemical decomposition of such compounds. [6]

The *Scope 2* is dealing with indirect emissions. The purchasing of electricity, required for the correct performing of the equipment and other production needs. At first sight, *Scope 2* can be investigated as one of the most important factors. The decreasing energy consumption not only reduces the production costs, but also makes the steelmaking more ecologically friendly. [6]

The *Scope 3* comprises emissions that are related to the production of all supply materials used during the processing. The amounts and types of these materials can widely range due to the production capacity and product mix. [6]

The European Commission demands to spread and integrate the Best Available Techniques for all the existing steelmaking routes. This document describes the ecological parameters and provides the reference data to improve the existing productions. Apart from that, the global ecological society is concentrated on other aims to decrease emission output from the global steelmaking. The industries flagship, known as ULCOS programme (Ultra-

Low Carbon Dioxide Steelmaking), supported by the European Commission and involving a consortium of 48 leading players in industry aims to reduce the CO_2 emissions in the steelmaking of today's best routes by at least 50%. The program is still under progress, and no implementation steps are scheduled yet but some achievements of the program were presented during the Steel Technology Platform Infodays (22.04.2015, Bruxelles, Belgium). The program looks initially at all the credible solutions, but fundamentally based on three sets of solutions:

- Keeping carbon-based processes and capturing CO_2 for storage, most likely geological storage initially.
- Improving existing pre-reduction technologies, for example the using of hydrogen for reducing iron ore into steel.
- Tapping into the large potential of sustainable biomass, which generates carbon at the same rate which is recovering CO_2 from the atmosphere by photosynthesis, to make steel. [12–14]

The energy efficiency of steelmaking facilities depends on the production route, material efficiency and steel product mix. But still the majority of all existing steelmaking routes contain the secondary metallurgy. Not much research was performed to estimate exactly this production segment concerning the point of view of CO_2 emissions. Thus, this thesis focuses on the evaluation of CO_2 emissions at secondary metallurgy and its savings potential.

1.2 CO_2 emissions in the secondary metallurgy

Historically, the Pirrin process – treatment of molten steel with synthetic slag – is the forerunner of modern secondary steelmaking, which was invented in 1933. In the decade 1950-1960 vacuum degassing processes came up due to the initial objective to reduce the hydrogen content in liquid steel to prevent the large forging-quality cracks. Then its objective also included lowering nitrogen and oxygen contents. Later the invented gas stirring offered additional advantages like homogenisation of temperature and composition of melt, as well as faster floating out of non-metallic particles and the reduction of carbon content. The growth of secondary steelmaking is closely associated with that of continuous casting. Initially a need for sequential production with continuous casting has provoked a demand for a buffer-unit between primary melter and the continuous casting machine (CCM). The high levels of interstitial impurities and inclusions in continuous casting made the secondary refining more important. Apart from the proper macrostructure and close control of the steel

temperature it is crucial to keep impurity level. Hence, such needs of temperature adjustment and high purity issues have led to the development of special furnaces. So secondary steelmaking has become an integral feature of modern steel plants. [15]

Basically, all the modern processes in secondary metallurgy are divided into: converter based processes and ladle based processes (**Figure 1-5**). Also these processes can be clustered as, processes performed under atmospheric pressure and under vacuum. According to the functionality, modern unites combine several processes. For example, some modern vacuum degassers (VD, **Figure 1-5**) are equipped with oxygen blowing and powder injection systems. This allows attaining desulfurization and decarburization in addition to the deoxidation function (VOD and VODC, **Figure 1-5**). [15,16]

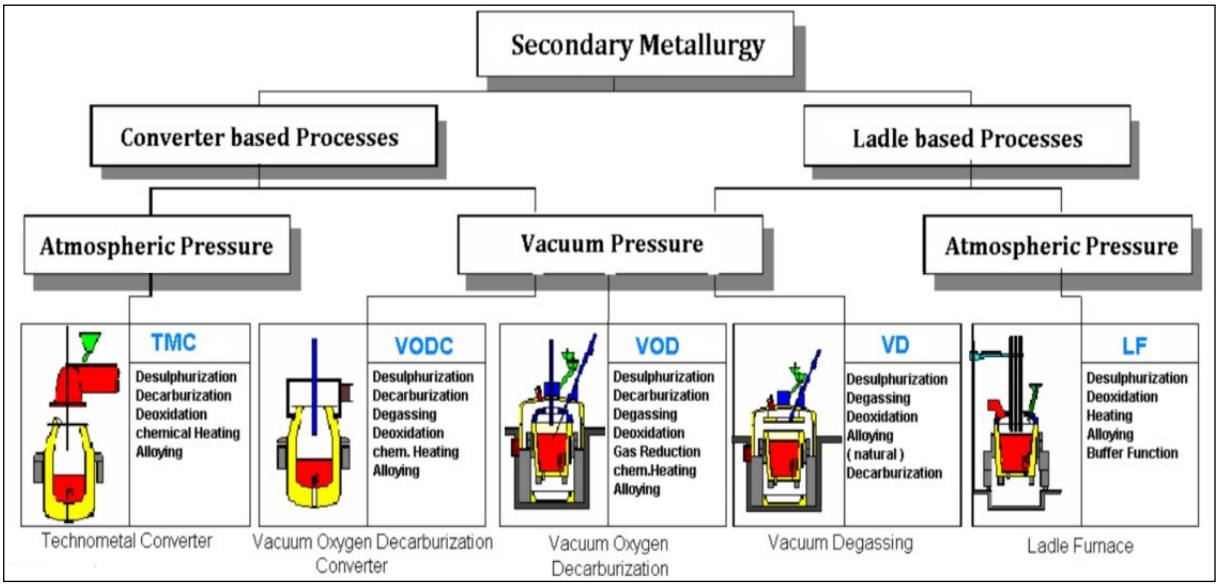

Figure 1-5: Classification of secondary metallurgy facilities. [16]

In general, secondary metallurgy processes excluding vacuum treatment are performed in the ladle furnace (LF). For this the ladle is placed on a stand under a cover, equipped with three graphite electrodes. These electrodes are connected to a three-phase transformer. The bottom part of ladle has a porous refractory plug, which is connected to argon supply pipe at the stand. The LF is also equipped with an addition hopper and injection lance on a hopper. During the LF-treatment electrodes are submerged into the slag and argon is blown through the bottom plug, providing the stirring. Alloying addition can be added through the hopper. [17]

Hence, apart from the buffer function, following operations of steel refinement can be done in the ladle: [17]

- steel phase separation from slag during tapping and casting,
- deoxidation and removal of undesirable elements like S, C,H, N further
- alloying of such elements as Mn, Cr, Si, Ti, V, besides
- setting of casting temperature (Adjustment of teeming temperature to optimal level),
- homogenisation of steel temperature and chemistry by means of inert gas stirring,
- decarburization and desulphurization and
- setting of special concentration ratios (Ti/N). [18]

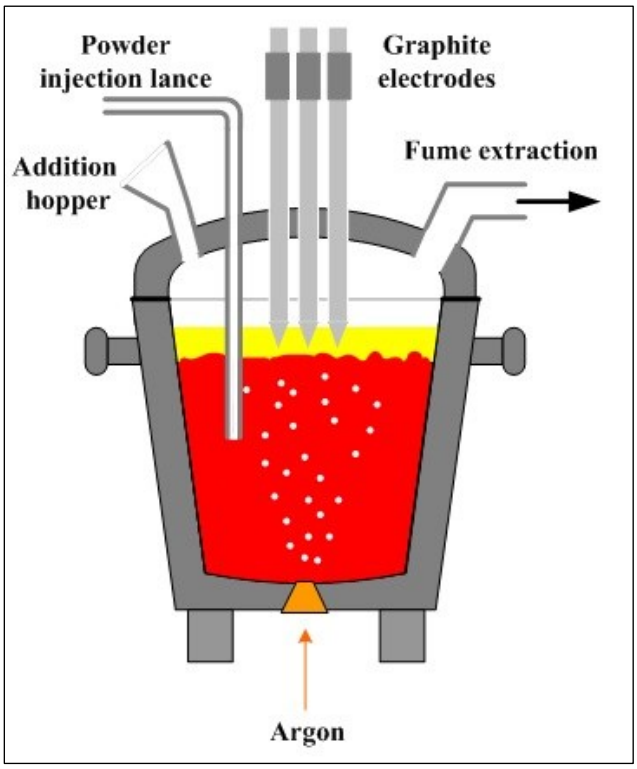

Figure 1-6: Overall view of typical ladle furnace (LF) [17]

First of all, it was necessary to define all the possible sources of CO_2 emissions during the steel stays in the ladle, to evaluate the emission input at the secondary metallurgy. A package of these sources has been verified during the negotiations with industrial partners – voestalpine Stahl Linz GmbH - a steel plant, located in Linz, Austria and RHI AG – a globally operating supplier of high-grade refractory products, systems and services, located in Vienna, Austria. Thus, the following estimation based on experience data, due to the real

operation practice of the corresponding steel plant. Any external by-sources like waste disposal and other outsourced activities were estimated. So, it is important to notice that, only installation ladle furnace (LF) and next operations were considered in the following calculations:

- alloying of crude steel by tapping from electric arc furnace (EAF),
- heating and purging with argon during LF-treatment,
- alloying of steel after treatment,
- casting on CCM and
- preheating treatment of the new lined ladle. [19]

In terms of secondary metallurgy, the first scope of emissions (*Scope 1*, **Figure 1-2**) includes emissions which are generated directly in the ladle and during the preheating treatment of the ladle after casting. The second scope (*Scope 2*, **Figure 1-2**) covers the purchased electricity during the LF-treatment, and the third (*Scope 3*, **Figure 1-2**) comprises emissions that are related to the purchasing of supply materials used during the processing.

Therefore, the *Scope 1* includes the direct emissions that are generated by:

- yield loss of carbon alloying,
- decomposition of carbonates, used for a slag generation further
- electrodes consumption in the process of LF treatment and
- combustion of natural gas during preheating of a new lined ladle. [20]

Electricity consumption during the LF-treatment relates to indirect emissions of *Scope 2*. In fact, the amount of purchased electricity correlates to the heaters capacity and required duration of heating, defined according to the actual temperature conditions. Thus, increasing of energy efficiency means at same time the reduction of indirect CO_2 emissions from *Scope 2*.

Indirect emissions of *Scope 3* are associated with purchasing of materials, such as alloying additions, refractory materials and stirring gas. All the values of these items were settled during the discussions with industrial partner. Further it was necessary to correlate the following study with the current production route, including all technological aspects. [20]

1.3 Evaluation principle

Besides the verification of the CO_2 emissions contribution this study is aimed to evaluate the potential for the reduction of these emissions based on the next assumed key factors:

- additions during tapping,
- ladle logistics and temperature losses under consideration of the steel contact time,
- treatment at the ladle furnace to compensate temperature losses and
- ladle preheating-treatment duration. [21]

Tapping from EAF presents the start point for the secondary metallurgy. During the tapping, the crude steel is alloyed by additions settled in the bottom of the ladle. The alloying additions are classified on two types:

1. alloying agents, aimed to adjust the composition of steel and
2. slag formers, aimed to generate the slag.

As long as proper slag is used in the ladle, secondary refinement allows to obtain high purity of the steel. It is also necessary to use an appropriate amount of the slag to refine the steel efficiently. Slag forming is a complicated process, dependent on many factors, but plays important role, like:

- steel desulphurization and deoxidation,
- purification of steel from non-metallic inclusions and
- thermal isolation. [22]

Usually slag in the ladle based on CaO, Al_2O_3, MgO and SiO_2. In practice appropriate slag component mix is depend on the produced steel. Also, it is important to notice the presence of MgO in the slag, aimed to improve the durability of the refractory lining of the ladle. The most common slag formers like lime, raw magnesite and alumina are used to generate the slag with required basicity ratio. This ratio includes specific proportion between the CaO, Al_2O_3 and MgO contents. [22]

Burnt lime is the main source for CaO in the slag. Alumina provides the required content of Al_2O_3. Raw magnesite is aimed to saturate the slag with MgO. At the same time raw magnesite contains a huge amount of carbon dioxide, due to the fact that it is a naturally occurring carbonate of magnesium - $MgCO_3$. Thus, saturation of the slag with MgO by raw

magnesite is accompanied with the decomposition of contained $MgCO_3$, which provides direct emissions of carbon dioxide. Potentially, raw magnesite can be substituted by burnt dolomite, also known as doloma. Originally it is a dolomite, burnt in a shaft kiln. The burning process significantly reduces the content of carbon dioxide. Remaining calcium and magnesium oxides occur at an almost stoichiometric ratio. So, by means of the substitution of raw magnesite on doloma it is possible to evaluate the potential for the reduction of direct emission during tapping. The assumed contents of calcium, magnesium and carbon oxides for the raw magnesite and doloma, as well as the comparisons are included in **Table 1-I**. [23]

Table 1-I: CaO-,MgO-, and CO_2 contents in slag formers [20]

Chemical compounds	Slag formers, [w.%]		Δ
	Doloma	Raw Magnesite	
CaO	56.0	11.5	+44.5
MgO	37.0	36.0	+1.0
CO_2	1.0	45.4	-44.4

Being the buffer unit for the production route, potentially LF can keep tapped steel as long as it is required. But the great problem of a ladle full of steel is heat losses. All these losses have to be compensated during the LF-treatment to fit the specified temperature requirements for casting on CCM. Therefore, minimizing the temperature loses correlated to time significance seems to be a key factor for increasing of energy efficiency and at the same time decreasing the indirect emissions from *Scope 2*. Thus, logistics of ladle were estimated, considering the different logistics of the ladle. Additionally, it was decided to estimate different configurations of the ladle: with and without cover - to evaluate the temperature losses under consideration of the steel contact time. [21]

Apparently, the combustion of natural gas to preheat the lining of the ladle during the ladle preheating treatment seems to be the most crucial source of direct emissions. Normally the duration of ladles preheating is specified by the volume of the ladle and capacity of the gas burner. But, real practice shows that this duration is often extended due to the actual production schedule. Hence, the preheating of the new lined ladle was also estimated. All these contributing factors, based on evaluation items and mentioned variations are given in **Table 1-II.** [21]

Table 1-II: Evaluation principle [21]

Contributing factor	Evaluation item	Variations	*Scope*
Additions during tapping	Slag saturation with MgO	by raw magnesite / by doloma	*1, 3*
Temperature losses under consideration of the steel contact time	Logistic of ladle	«good» - short delays / «poor» - long delays	*2*
	Configurations of ladle	with no cover / with cover	
Preheating of the ladle	Duration	9±1hour	*1*

1.4 Task assignment (statement)

For the verification of the amount of CO_2 emissions, it is necessary to describe the current production route by an industrial partner.

The temperature of crude steel, tapped from EAF is 1640°C, the heat size is 170 tons. The tapping takes 5 minutes. The chemical composition of steel before tapping as well as requirements to the composition of steel before casting are included in **Table 1-III**. Also, the steel will be alloyed twice to fit these demands. First alloying is performed during the tapping. It was assumed, that no slag from EAF was poured into the ladle. So the amount of alloying additions is also specified to generate the slag with "**LF1**" chemical composition. When the first alloying is completed, steel has to be treated in LF. After that, the second alloying is performed to fit "**LF2**" chemical composition requirement. The following reduction of slag before the casting on CCM was also considered in such a way that after reduction steel and slag composition would suit the "**CCM**" composition specification. [19]

Table 1-III: Steel and slag composition requirements before tapping (EAF), after first alloying (LF1), after second allying (LF2) and before casting (CCM) [19]

Composition of steel, [w.%]							Composition of slag, [w.%]						
	C	Si	Mn	P	S	Al		FeO	MnO	CaO	Al_2O_3	SiO_2	MgO
EAF	0.04	-	0.10	0.020	0.01	-	**EAF**	-	-	-	-	-	-
LF1	0.10	0.18	0.75	0.022	0.01	0.05	**LF1**	6	4	40	23	13	14
LF2	0.12	0.20	0.80	0.022	0.01	0.038	**LF2**	4	2	40	26	15	12
CCM	0.12	0.20	0.80	0.022	0.01	0.030	**CCM**	2	1	40	30	14	13

Taking into account contribution factor "additions during tapping" from **Table 1-II**, it was assumed to develop the alternative alloying concept, using a doloma for the slag saturation with MgO. The optional concept has to suit the same steel and slag composition requirements mentioned in **Table 1-III**.

Thus, the CO_2 emission input has to be evaluated based on the two possible alloying concept variations:

1. current alloying concept with using raw magnesite – "**RM**-concept" and
2. optional alloying concept with using doloma – "**DL**-concept". [19]

Relying on the real operation practice, it was decided to consider possible delays during next time segments to evaluate the temperature losses due to the:

1. waiting time after EAF tapping and before start of LF-treatment (**WT-1**) and
2. waiting time after LF-treatment finished and casting started (**WT-2**). [19]

In cases of "good" logistic, time segments **WT-1** and **WT-2** were set for 20 and 15 minutes respectively. In cases of "bad (poor)" logistic, they were set for 90 and 30 minutes (**Figure 1-7**). Apart from that, it was decided to evaluate the potential of the decreasing heat losses by means of using a ladle cover during these two time segments. All the geometry dimensions and lining configurations of the ladle were taken out of the internship protocol, provided by the industrial partner. [21]

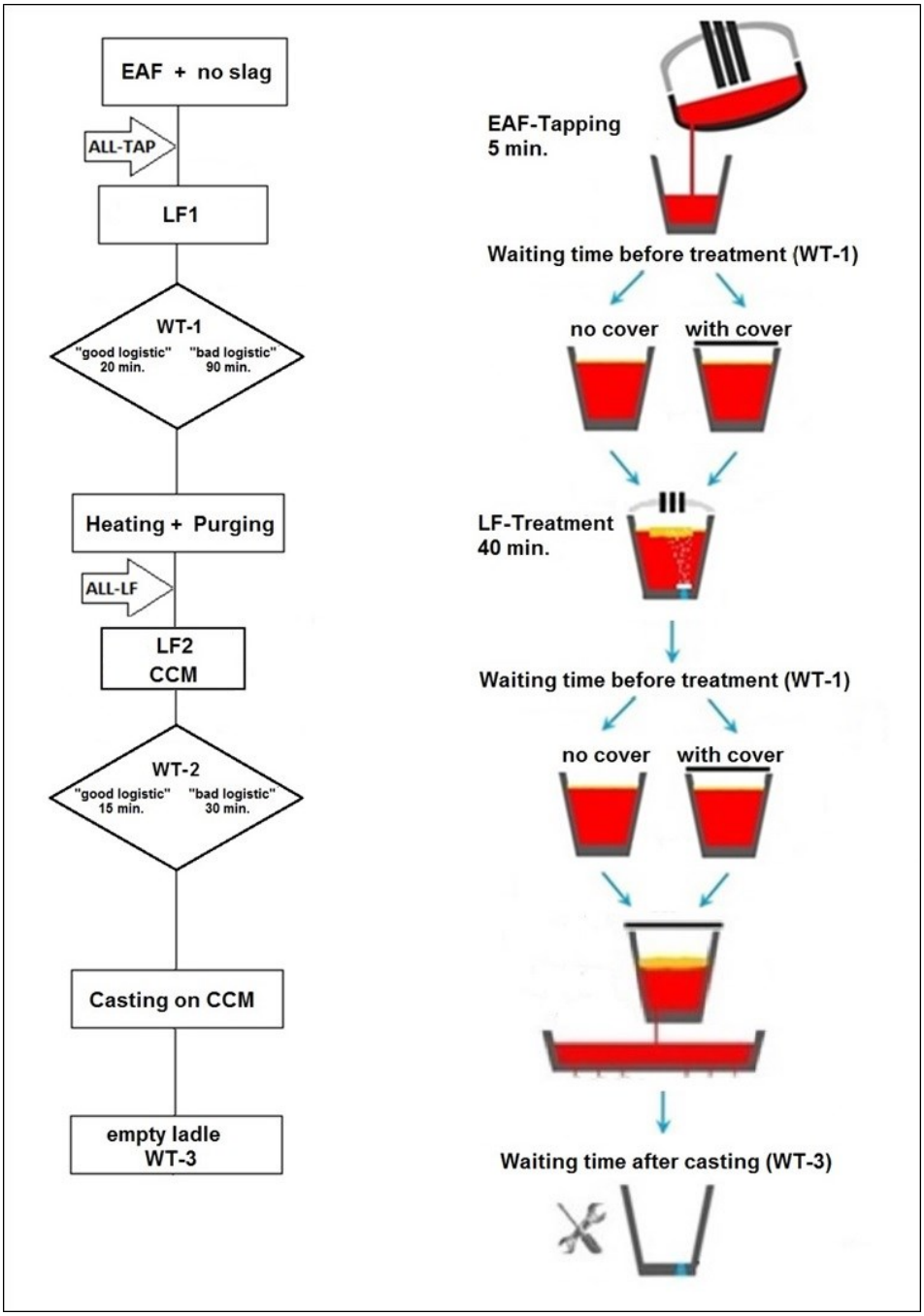

Figure 1-7: Flow chart of evaluation for corresponding production route [21]

The duration of the LF-treatment was set for 40 minutes. And for the entire treatment, steel is purged with argon. The duration of heating is specified by the heating rate +4°C/min and the amount of temperature to compensate to fit the casting temperature 1560°C. It is crucial to notice, that the amount of temperature losses to be compensated during LF-treatment also includes the temperature losses during the whole cycle, even when the ladle is empty after casting (**WT-3**). This segment was set for 40 minutes – 20 minutes for service and 20 minutes as waiting time before EAF-tapping. [19]

Thus, these logistic assumptions including the mentioned variations are aimed to evaluate the quantity of the electrical energy for the LF-treatment, to compensate the sum of losses during **WT-1**, **WT-2** and **WT-3** as well as all the heat losses, caused by alloying. The potential of the energy savings during treatment also means the savings of indirect emissions from *Scope* 2 (**Figure 1-2**).

The corresponding production route lifetime of the ladle lining is 110 heats, and no service is performed during this period. Therefore, ladle preheating treatment is performed only for new lined ladles and normally takes 8 hours to preheat the lining up to 1100°C. The variations, mentioned in **Table 1-II**, are aimed to evaluate the CO_2 emission input by 9±1 hour durations. Thus, all the mentioned logistic assumptions, with corresponding designations are included in the **Figure 1-8**. [21]

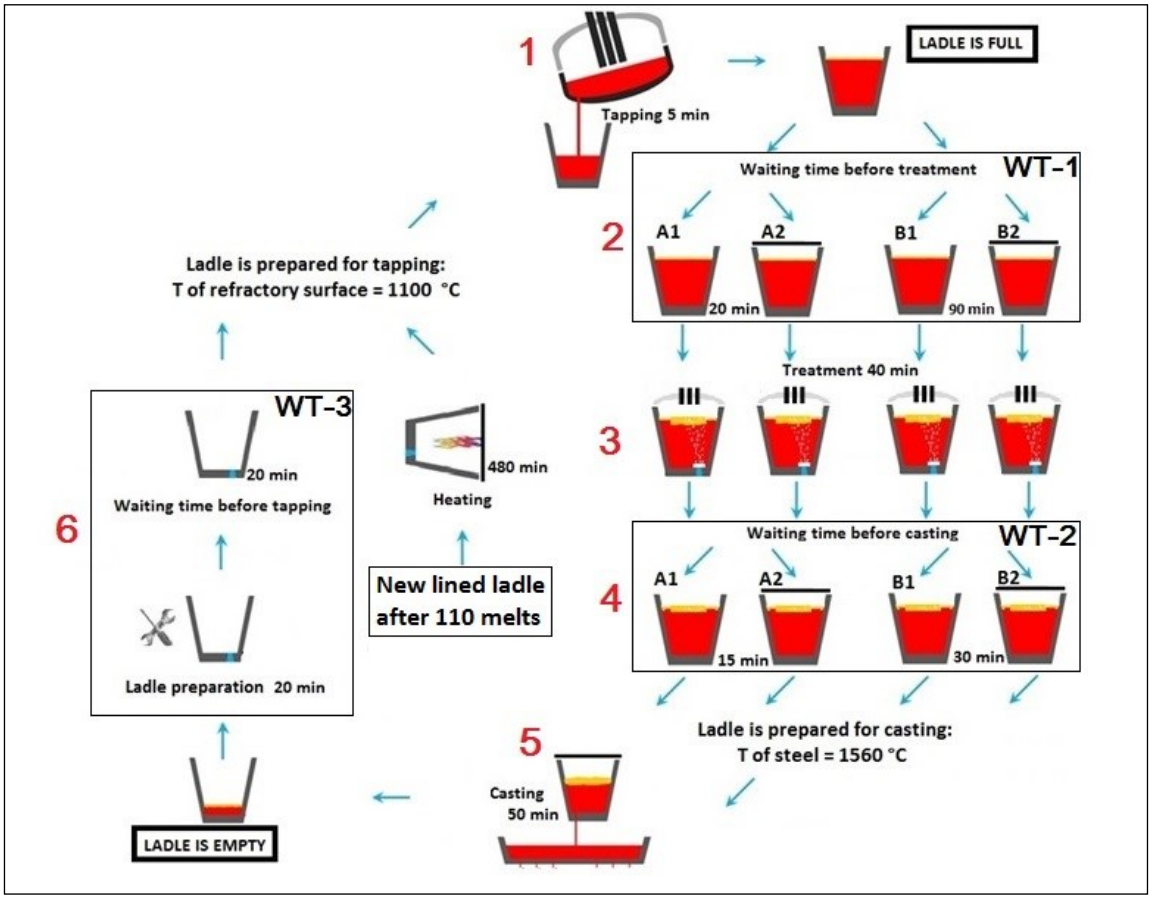

Figure 1-8: Logistic assumptions for the estimation [21]

2 Mathematical formulation

As it was mentioned before, the tapping of crude steel from EAF is the starting point for the secondary metallurgy, furthermore for the following calculations. Also the first alloying is performed at the same moment. First of all it was necessary to develop a mass- and energy balance, based on the provided alloying concept requirements and a list of alloying additions. Moreover, this allowed the evaluation of the temperature losses, caused by alloying, considering the steel and slag chemistry. The development of the mass and energy balance for the optional alloying concept using doloma makes it possible to estimate the potential to reduce the direct emissions by alloying.

Secondly it was crucial to estimate the heat losses of the ladle full of steel under consideration steel contact time, based on the corresponding ladle parameters. The detailed drawings of the ladle, including lining parameters were provided by the steel plant. Additionally, the calculations for the alternative configuration of the ladle (using a cover) provided important values to assess the potential to reduce the temperature loss, the indirect emissions and electricity during the LF-treatment.

Very few systematic investigations of such temperature changes could be found in the literature. Thus, during the internal communication, it was decided to divide all the heat losses during the steel contact time at the secondary refinement into two groups:

- losses caused by alloying and
- losses caused by ladle parameters. [21]

The alloying concept and the mass-, energy- and heat balances were developed considering the steel and slag chemistry, basics of thermodynamics and approved by industrial operation practice.

2.1 Mass balance of corresponding production route

2.1.1 Developing the alloying concept

First of all, for the formulation of the mass balance it was necessary to create a list of alloying agents, including their chemical composition. Thus, after the negotiation with the industrial partner, the following list of additions (**Table 2-I**) was considered for the development of the alloying concept. The chemical compounds, contained in the alloying agents, but not mentioned in requirements are marked as “balance” item. [21]

Table 2-I: List of alloying additions and slag formers [21]

Chemical elements and compounds		**Alloying additions, [w.%]**						
		FeSi	FeMn	Lime	Raw Magn.	Alumina	Al	Coke
Steel composition formers	C	0.17	7.03	-	-	-	0.00	97.50
	Si	71.06	0.10	-	-	-	0.80	0.00
	Mn	0.24	78.20	-	-	-	0.00	0.00
	P	0.02	0.07	-	-	-	0.00	0.00
	S	0.00	0.01	-	-	-	0.00	0.50
	AL	1.66	0.01	-	-	-	99.08	0.00
	O	0.00	0.00	-	-	-	0.00	0.00
	Fe	22.20	13.80	0.06	-	-	0.12	0.80
Slag composition formers	FeO	-	-	0.15	3.50	-	-	-
	MnO	-	-	0.04	2.80	0.20	-	-
	SiO_2	-	-	0.20	0.60	1.00	-	-
	Al_2O_3	-	-	0.30	0.20	71.16	-	-
	CaO	-	-	87.40	11.50	23.35	-	-
	MgO	-	-	6.40	36.00	2.53	-	-
CO_2		-	-	-	45.40	-	-	-
Balance		4.64	0.79	4.17	0.00	1.76	-	1.20
Sum		100.00	100.00	100.00	100.00	100.00	100.00	100.00

First it was necessary to calculate an alloying mass ($m_{alloying\,(i)}$) for each chemical element (i). The alloying mass presents the summarised multiplications of weight content of the corresponding chemical element ($w.\%_{(i)}$) with the corresponding mass of alloying agent (j) respectively. [24]

$$m_{alloying\,(i)} = \sum w.\%_{(i)}\, j \cdot m_j \tag{2-1}$$

For example, the alloying mass of carbon, calculated using equation (2-1), is equal to 160.14 kg (**Table 2-II**). The masses of other alloying agents were calculated in the same manner due to the composition requirements from **Table 1-III**.

Table 2-II: Example of alloying mass calculation for carbon

Alloying agent	FeSi	FeMn	Al	Coke	Alloying mass of C, [kg]
C content, [w.%]	0.17	7.03	0.00	97.50	160.14
Mass, [kg]	625	1 500	300	55	

The primary input-materials for steelmaking are iron containing elements such as carbon, silicon, manganese, phosphorus and sulphur. As a rule, contents of these elements must be at least partially removed, in order to achieve the desired crude steel- or steel composition. Hence, oxidation reactions are aimed to remove these tramp elements from the crude steel, since the respective elements have a higher affinity for oxygen than iron. The resulting oxidation products are separated from the molten steel and excreted with the exception of CO in the slag. [25] As for the alloying model accuracy, it has a direct impact on the quality of steel and the model precision depends mainly on the recovery rate of the alloying elements calculation. In the refining (alloying) process at the ladle furnace, there are many factors that affect recovery rate of alloying elements, such as the steel temperature, oxygen level, slag condition and so on. Their relationship is very complicated. Thus, it was decided to take into account the recovery rate values, taken out of the lecture “Ferrous-Steel-Metallurgy II, Mod. 2” included in the bachelor program of Montanuniversitaet. These rates differ for the alloying by EAF-tapping and alloying in LF. Alloying in LF is associated with higher recovery rate in comparison with alloying during the EAF-tapping (**Table 2-III**). [24,26]

Table 2-III: Recovery rates of alloying agents [21,24]

Elements	Recovery rate of alloying, [%]	
	by EAF-tapping	in LF
C	66	95
Si	69	98
Mn	66*	95
P	69	98
S	56	80
AL	30*	95
O	70	100
Fe	70	100

*During the negotiations it was decided to adapt the recovery rates of Mn and Al. Real operation practice and absence of slag, coming from EAF allow to admit these adaptions as acceptable. [21]

Thus, to calculate the alloyed mass ($m_{alloyed}$) of each element, it is necessary to multiply the alloying mass ($m_{alloying}$) of each component with the corresponding recovery rate ($r.\%$), as it is notice in equation (2-2). [24]

$$m_{alloyed_{(i)}} = \frac{m_{alloying_{(i)}} \cdot r.\%_{(i)}}{100} \tag{2-2}$$

The sum of alloyed mass of each element ($m_{alloyed}$) with the mass of corresponding element in the steel before alloying ($m_{before\ alloying}$) represents the mass of element in steel after alloying ($m_{after\ alloying}$). The composition of steel before alloying is noticed in **Table 1-III**. Mass of steel ($m_{EAF-steel}$) before alloying was assumed as 170 tons.

$$m_{alloyed_{(i)}} + m_{before\ alloying_{(i)}} = m_{after\ alloying_{(i)}} \tag{2-3}$$

where

$$m_{before\ alloying_{(i)}} = w.\%_{(i)} \cdot m_{EAF-steel} \tag{2-4}$$

Thus, all the required masses of each alloying agent from **Table 2-I** were respectively calculated using an iteration method to fit the required composition of steel after tapping (LF1, **Table 1-III**).

Table 2-IV: Calculation of required amount of additions during alloying by tapping

Composition of steel - EAF			Alloying mass	Recovery rate	Composition of steel - LF1		
	[w.%]	[kg]	[kg]	[%]		[w.%]	[kg]
C	0.04	68	160.14	66	C	0.10	173.7
Si	0.00	0	448.03	69	Si	0.18	309.1
Mn	0.10	170	1 174.53	66	Mn	0.75	1 285.8
P	0.02	34	1.18	69	P	0.02	34.8
S	0.01	17	0.40	56	S	0.01	17.2
AL	0.00	0	307.69	30	AL	0.054	92.3
O	0.06	102	0.00	70	O	0.002	4.1
Fe	99.77	169 609	347.03	70	Fe	98.8	169 851.9
Sum	100	170 000	1847.3		Sum	100	171 847.3

Thus, the mass of steel after tapping increased by 1847.3 kg (**Table 2-IV**) to fit the required composition LF1 (**Table 1-III**) during the first alloying by tapping. The amount of alloying agents are included in **Table 2-V**, also these values are recalculated to the special value, by dividing the corresponding masses of the mass of steel before alloying – 170 tons.

Table 2-V: Amount of alloying agents during alloying by tapping in kg/t_{ls}

	FeSi	FeMn	Al	Coke
Mass of alloying agent, [kg]	625	1 500	300	55
Special value, [kg/t_{ls}]	4.1	9.0	1.7	0.5

The unrecovered part (**Table 2-III**) of alloying agents along with the rest of the added slag formers (**Table 2-I**) would generate the slag. The mass of slag, generated by oxidation of alloying agents was calculated basing on the following reactions:

$$\left[Si\right]+2[O]\rightarrow\left(SiO_2\right) \tag{2-5}$$

$$\left[Mn\right]+[O]\rightarrow\left(MnO\right) \tag{2-6}$$

$$2\left[Al\right]+3[O]\rightarrow\left(Al_2O_3\right) \tag{2-7}$$

$$\left[Fe\right]+[O]\rightarrow\left(FeO\right) \tag{2-8}$$

Thus, the total mass of each oxide in slag (o) presented as a sum of alloying part and oxidised part (equation (2-9)). Alloying part is the sum of oxides, contained in the added slag formers (j), is calculated analogical to equation (2-1). The mass of oxidised part of each metal (m) during alloying was calculated taking into account its recovery rate, noticed in **Table 2-III** and molar masses of the corresponding metal (m) and generated oxide (o).

$$m_{(o)\,in\ slag}=m_{alloying_{(o)}}+m_{oxidated_{(o)}} \tag{2-9}$$

$$m_{alloying\,(o)}=\sum w.\%_{(o)}\,j\cdot m_j \tag{2-10}$$

$$m_{oxidated_{(m)}}=\frac{m_{alloying_{(m)}}\cdot\left(100-r.\%_{(m)}\right)}{100}\cdot\frac{M_o}{M_m} \tag{2-11}$$

The calculation of alloying additions and slag former amounts were performed synchronously using an iteration method to fit the “LF1” steel and slag composition requirements from **Table 1-III**. The second alloying, performed in LF after treatment, was calculated in the same manner, considering the other recovery rates for the corresponding

elements for the alloying in LF (**Table 2-III**). In addition, to the second alloying the reduction of generated slag was taken into account. [21]

It was assumed, that such oxides as MnO and FeO would be reduced by Al and Si due to theirs chemical activity. Thus, slag reduction implies a decreasing of Al and Si content in steel composition, furthermore the increase of alumina content in the slag. The reduction of FeO by Si was also taken into account, which is associated with the increasing of Fe content in steel composition and decreasing of SiO_2 in the slag. Thus, the calculation of slag reduction was based on the combination of next chemical reactions: [21]

$$2[Al]+3(MnO)\rightarrow 3[Mn]+(Al_2O_3) \tag{2-12}$$

$$2[Al]+3(FeO)\rightarrow 3[Fe]+(Al_2O_3) \tag{2-13}$$

$$[Si]+2(FeO)\rightarrow 2[Fe]+(SiO_2) \tag{2-14}$$

The ratio of molar mass of each component to its mass is equal to its oxidised as well as its reduced form. Thus, synchronously taking into account the masses of oxides to reduce (r) it is possible to calculate the masses of recovered metals, as well as generated oxides (g). [27]

$$\frac{m_r}{M_r}=\frac{m_g}{M_g} \tag{2-15}$$

It was assumed that, 70% of FeO amount in the slag is reduced by Al, and the rest by Si. Thus, taking into account the known required masses of oxides to generate, it is possible to adjust the masses of previously calculated amounts of oxides to reduce the slag. Basing it on equation (2-15), correlated to the system of chemical reactions (2-12) - (2-14) and composition requirements from **Table 1-III**, masses of the mentioned oxides were calculated iteratively. Considering the masses adjustment, the next amounts of oxides, defined to reduce and to generate during the slag reduction are included in **Table 2-VI**. Apart from that, these reactions were synchronously considered with preceding alloying to adjust the required amount of additions due to the predicted slag reduction. The detailed mass distribution of each reduced and recovered oxide during slag reduction is mentioned in **Table 2-VII**.

Table 2-VI: Amount of slag components to reduce and to generate

Oxides	in slag before reduction	in slag after reduction	to reduce	to generate
	[kg]			
FeO	159.01	46.76	112.24	
MnO	98.15	23.38	74.76	
AL_2O_3	553.33	693.84		140.51
SiO_2	307.78	381.92		74.14

Table 2-VII: Distribution of mass changing by slag reduction due to the chemical reaction [19]

Oxides during the slag reduction LF2 to CCM	[kg]	[w.%]
FeO in slag before reduction	159.01	6.80
due to reduction by Al	-72.96	-3.12
due to reduction by Si	-39.28	-1.68
MnO in slag before reduction	98.15	4.20
due to reduction by Al	-74.76	-3.20
SiO_2 in slag before reduction	307.78	13.16
due to reduction of FeO	+23.73	+1.02
AL_2O_3 in slag before reduction	553.33	23.67
due to reduction of FeO+MnO	+140.51	+6.01

Thus, based on the calculation, the mass of slag due to the reduction decreased at 22.76 kg from 2338.18 to 2315.41 kg, (**Table 2-VIII**). In the same table you can see the special value – relation of total mass of the slag to the total mass of the alloyed steel. Also in **Table 2-VIII** some basicity relations are provided. The relation, marked as B_2 ratio is equal to ratio between CaO to SiO_2 contents. The ratio B_4 is equal to the ratio between the sum of CaO with MgO contents to the sum of SiO_2 and Al_2O_3 contents in the slag. The relation between CaO and Al_2O_3 is marked as ratio C to A. [28]

Table 2-VIII: Mass change of the slag due to the reduction after alloying in LF and basicity ratios [19]

Mass of slag before slag reduction	2 338.18	[kg]
reduced FeO+MnO	-187.01	
recovered SiO_2+Al_2O_3	+164.24	
Mass of slag after slag reduction	2 315.41	
Δ mass of slag due to reduction	-22.76	
Special value	13.45	[kg/t_{ls}]
Ratio B_2: CaO / SiO_2	2.75	
Ratio B_4: CaO+MgO / SiO_2+Al_2O_3	1.19	
Ratio C to A: CaO / Al_2O_3	1.31	

After the final settling of the alloying concept, including the amount of generated and reduced slag, it was necessary to consider the gases and oxygen activity in the steel by alloying. For this, it is necessary to assume, that activity of oxygen (a_o) approximated closely by its partial pressure (P_i), because reactions take place at atmospheric pressure. This activity coefficient was set as 1. [29]

Developing gas compounds by corresponding route during alloying is performed by oxidizing carbon. Regarding to the issue of this study, it was assumed to consider full oxidation of carbon to carbon dioxide to predict a "worst case scenario". Thus, the amount of CO_2, cause by alloying was calculated as a sum of an unrecovered part of carbon by alloying with compounded carbon dioxide and coming with agents through the alloying, mostly via raw magnesite. The detailed results of calculated direct CO_2 emissions due to alloying are provided in **Table 2-IX**. [21]

$$m_{oxidated_{(C)}} = \frac{m_{alloying_{(C)}} \times \left(100 - r.\%_{(C)}\right)}{100} \cdot \frac{M_{CO_2}}{M_C} + \sum w.\%_{(CO_2)} i \cdot m_i \qquad (2\text{-}16)$$

Where $m_{alloying_{(c)}}$ – alloying mass of carbon,

$r.\%_{(C)}$ – recovery rate of carbon during alloying by tapping,

M_{CO_2} , M_C – molar masses of carbon dioxide and carbon,

i – alloying agent,

$w.\%_{(CO_2)}\ i$ – weight content of carbon dioxide in alloying agent and

m_i – mass of corresponding alloying agent.

Table 2-IX: Generation of direct CO_2 emission, caused by alloying for the current concept using of raw magnesite for the slag saturation with MgO [21]

Direct CO_2 emission due to alloying	by tapping	in LF	Sum	
	[kg]			[kg/t_{ls}]
CO_2 generated by carbon oxidation	199.64	6.92	526.8	3.06
compounded CO_2 from alloying agents	318.96	1.28		

Regarding the oxygen activity, it was necessary to analyse all chemical processes, in which oxygen is involved. The content of oxygen in the crude steel was set as 600 ppm. It was assumed to define a target value of oxygen after alloying basing on required aluminium content after alloying and its deoxidation potential. [24]

$$K' = [Al]^2 \times [O]^3 = 3.3 \cdot 10^{-14} \text{ at } 1600°\text{C} \tag{2-17}$$

$$[O]_{after\ alloying\ by\ tapping} = \sqrt[3]{\frac{K'}{[Al]^2}} = \sqrt[3]{\frac{3.3 \cdot 10^{-14}}{0.05^2}} = 2.363\ ppm \tag{2-18}$$

$$[O]_{after\ alloying\ in\ LF} = \sqrt[3]{\frac{3.3 \cdot 10^{-14}}{0.03^2}} = 3.322\ ppm \tag{2-19}$$

Where $[Al]$ – target value of aluminium in steel after completed alloying, ppm

$[O]_{after\ alloying\ by\ tapping}$ – target value of oxygen in steel after alloying by tapping, ppm

$[O]_{after\ alloying\ in\ LF}$ – target value of oxygen in steel after alloying in ladle furnace, ppm

The two calculations were performed, taking into account required aluminium contents after alloying by tapping – equation (2-18) and in LF – equation (2-19). Thus, it was necessary to take into account all the chemical processes, in which oxygen is involved. Oxygen is required for slag generation and CO_2 generation. Also some oxygen is chemically bonded in oxides with slag formers by alloying. Thus, taking into account these items as well as primary oxygen content before alloying and target value of oxygen content after alloying, it is possible to calculate the missing amount. All the considered sources of oxygen distribution are included in **Table 2-X**.

The amount of oxygen dissolved in crude steel were assumed as 600 ppm, the contents after alloying were calculated with equations (2-18) and (2-19). These values were recalculated in kg, based on the corresponding masses of steel. Thus, the crude steel after tapping contains 102 kg of oxygen and 4 kg of oxygen which will be dissolved in steel after alloying. These values are included in **Table 2-X**.

The amount of oxygen coming from slag formers was calculated basing on the molar mass ratios, analogical to equation (2-15) due to the corresponding mass of each slag former addition, which contains oxygen. Thus, 165.04 kg of oxygen is included in oxides, coming from slag formers during alloying by tapping. The sum of this amount with the previous item - oxygen dissolved before alloying - makes the total existing oxygen **Table 2-X**.

The required oxygen is presented by the sum of amounts required for slag and CO_2 generation with regard to the equilibrium due to Al-deoxidation (target value of oxygen content after alloying). Taking into account the calculated mass of generated carbon dioxide in **Table 2-IX** and the molar mass ratio (equation (2-15)), it is possible to define the amount of oxygen, required for CO_2 generation. Using the same molar mass ratio (equation (2-15)) and calculated masses of oxides in the slag, it is possible to define the amount of oxygen, required for the slag generation.

It is obviously clear, that amount of required oxygen is twice higher than amount of existing oxygen. It was assumed to compensate the missing amount by oxygen from of the surrounding air. All the values are included in **Table 2-X**.

Table 2-X: Oxygen balance during alloying [19]

Amount of O_2		[kg]		
		by tapping	in LF	Sum
existing	dissolved in steel	102.0	4.1	267.0
	contained in slag formers	165.0	0.0	
required	for CO_2 generation	145.2	5.0	549.6
	for slag generation	397.5	1.9	
	equilibrium due to Al-deoxidation	4.1	5.7	5.7
missing, taken out of the air		279.7	2.9	288.2
Balance		0.0	0.0	0.0

Thus, the alloying concept was defined by summing the amounts of alloying additions and slag formers. This concept, using a raw magnesite for the slag saturation with MgO is already implemented in the production route of the estimated steel plant. All the data was confirmed by the industrial partner, based on the real experience data, including all the adaptions due to the steel and slag chemistry. The calculated amounts of each alloying additions and slag formers are included in **Table 2-XI**. Also these values were recalculated to the special values in kg/t_{ls}, due to the corresponding mass of steel.

Table 2-XI: The current alloying concept for corresponding production route [19]

Mass of alloying addition	Unit	FeSi	FeMn	Al	Coke	Lime	Raw Magn.	Alumina
Alloying during tapping		625	1 500	300	55	800	680	200
Alloying in LF	[kg]	75	50	0	35	100	0	00
Sum		700	1 550	300	90	900	680	200
Special value	[kg/t_{ls}]	4.1	9.0	1.7	0.5	5.2	4.0	1.2

Hence, in **Figure 2-1** can be seen the illustration of current alloying weight content charts. On the left part of the figure are the charts symbolizing the weight content change of some steel components, on the left some compound contained in the slag. The weight content change is correlated to the production step and meets the requirements to the steel and slag composition, mentioned on the **Table 1-III**.

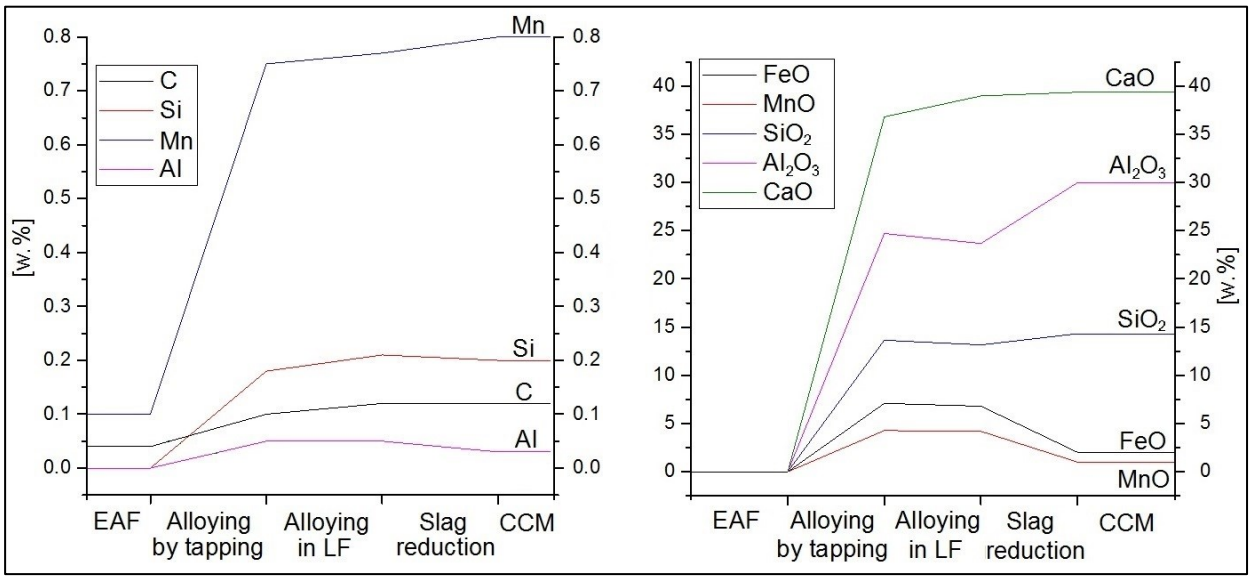

Figure 2-1: The weight content change of the steel and slag composition per production step

2.1.2 Developing the optional alloying concept

Based on the CO_2 emission contributing factor mentioned in **Table 1-II**, it was decided to calculate the alternative alloying concept, to evaluate the reduction potential. The evaluation item was assumed as slag saturation with MgO, which was originally performed by using raw magnesite. The optional variation of MgO carrier was calculated with the use of doloma.

The most common use for dolostone is in the construction industry. It is crushed and measured for use as a road base material, an aggregate in concrete and asphalt, railroad ballast, rip-rap or fill. Dolomite's reaction with acid also makes it useful. It is used for acid neutralization in the chemical industry. Furthermore, it is used as a sintering agent and flux in metal processing, and as an ingredient in the production of glass, bricks and ceramics. Basically, doloma is produced by heating of dolomite stone - ($CaMg(CO_3)_2$). [30–32]

$$CaMg\left(CO_3\right)_2 + heat \rightarrow CaO.MgO + 2CO_2 \tag{2-20}$$

Theoretically dolomitic lime should be a stoichiometric mixture of CaO and MgO, i.e. 58 w.% of CaO and 42 w.% of MgO. In practice, because of impurities and differing levels of dolomitisation, commercial products normally contain about 35 w.% of MgO. When dolomite is heated at a high temperature it loses its reactivity and the product is known as burnt dolomite. On **Figure 2-2** you can see a visual difference between dolomite stone and burnt dolomite. [30–32]

Figure 2-2: Comparison of dolomite stone and burnt dolomite [33]

The smaller content of carbon dioxide (**Table 2-XII**) due to the issue of this study can be considered as advantage. But the relative higher price comparative to the raw magnesite is a reason to evaluate the sustainability of such a substitution. Apart from that, chemical compositions of these slag formers are differing not only in carbon dioxide. The chemical compositions of doloma and raw magnesite are compared in **Table 2-XII**.

Table 2-XII: Comparison of chemical composition of raw magnesite and doloma [19]

Chemical compounds	Slag generators, [w.%]		Δ
	Doloma	Raw Magnesite	
FeO	0.0	3.5	-3.5
MnO	0.0	2.8	-2.8
SiO_2	1.5	0.6	+0.9
Al_2O_3	0.2	0.2	-
CaO	56.0	11.5	**+44.5**
MgO	37.0	36.0	+1.0
CO_2	1.0	45.4	**-44.4**
balance	4.3	1.8	-
total	100.0	100.0	-

The alternative alloying concept using doloma was developed identically to the current alloying concept mentioned before. The values of additions were balanced to fit the same steel and slag composition requirements, noticed in **Table 1-III**. Thus, amounts of alloying agents and slag generators for alternative concept are included in **Table 2-XIII**.

Table 2-XIII: Alternative alloying concept with using doloma for the slag saturation with MgO

Mass of alloying addition	Unit	FeSi	FeMn	Al	Coke	Lime	Doloma	Alumina
Alloying during tapping	[kg]	625	1 500	300	55	415	750	200
Alloying in LF		75	65	0	30	100	0	0
Sum		700	1 565	300	85	515	750	200
Special value	[kg/tls]	4.1	9.1	1.7	0.5	3.0	4.4	1.2

After balancing the alternative alloying concept it was decided to compare both concepts to realise potential difference. The comparison was performed via special values of each alloying addition in kg per t_{ls}. The most significant difference is the amount of lime addition –

the alternative alloying concept requires 2.2 kg/t_{ls} less than the concept with the usage of raw magnesite for the slag saturation with MgO.

Table 2-XIV: Comparison of alloying addition masses due to the current and potential alloying concept

Alloying concept	Alloying addition masses due to the concept [kg/t_{ls}]						
	FeSi	FeMn	Al	Coke	Lime	MgO-supplier	Alumina
with raw. magnesite - RM	4.1	9.0	1.7	0.5	5.2	4.0	1.2
with doloma - DL	4.1	9.1	1.7	0.5	3.0	4.4	1.2
Δ	0.0	-0.1	0.0	0.0	+2.2	-0.4	0.0

The estimation of direct CO_2 emissions due to alloying for the alternative alloying concept was performed in the same manner – via equation (2-16). In the **Table 2-XV** you can see a comparison of results for current and alternative alloying concepts. Therefore, it is possible to reduce the direct CO_2 emission more than twice, by means of the substitution of the raw magnesite in doloma for the slag saturation with MgO, by the current production route. But for the meaningful estimation of the savings potential, it is necessary to take into account sources of indirect emissions (**Figure 1-2**).

Table 2-XV: Comparison of direct emission due to alloying by current and alternative alloying concepts

Alloying concept	Total direct CO_2 emission due to alloying	
	[kg]	[kg/t_{ls}]
Concept with raw. magnesite - RM	527	3.06
Concept with doloma - DL	220	1.27
Δ	307	1.8

2.2 Heat balance of corresponding production route

The next step of the assessment of the current production route is the development of heat balance, aimed to define the total heat losses. As it was mentioned before, it was assumed to cluster the heat losses at the secondary metallurgy into two groups. First group includes the "internal" losses, caused by alloying. Second group includes the "external" losses, associated with radiation heat loss from the ladle to the surrounding area. Both groups of heat losses were estimated consecutive: firstly, the "internal", caused by alloying and then the "external" losses. All the losses were calculated in Joules (J) and then recalculated to the Celsius degree (°C) due to the heat capacity and emission values of corresponding bodies/surfaces (liquid steel, refractory layers and steel shell of the ladle).

Furthermore, the total amount of heat losses would assess the amount of steel temperature to compensate before casting at CCM. This consequently allows defining the heating duration during the LF-treatment and its energy consumption. Thus, it would be possible to evaluate the amount of indirect CO_2 emissions, associated with purchasing the required electricity and its savings potential due to the assumed assumptions, noticed on the **Figure 1-8**. [28]

2.2.1 Evaluation of heat loses by alloying

Every of mentioned chemical reactions by alloying have its energy and heat potential. Thus, to estimate the alloying process from viewpoint of the heat generation and heat loses, it was necessary to analyse the heat influence of each addition due to calculated alloying concept. The thermotechnical parameters of tapped crude steel represent the start condition of the heat balance. The temperature of steel before tapping ($T_{steel-tapping}$) was set as 1640°C, the heat size ($m_{crude\ steel}$) - 170 tones. The heat capacity (c_p) of crude steel was assumed as 840 J/kgK. The equation (2-21) was used to define an amount of heat of the steel before alloying - $H_{crude\ steel}$. [27]

$$H_{crude\ steel} = \left(m_{crude\ steel} \cdot T_{steel-tapping} \cdot c_p \right) \tag{2-21}$$

It is well known, that according to the heat effect, all the chemical reactions are divided on two types: exothermic and endothermic. In corresponding concept exothermic reactions are performed by oxidation reactions for the metal phase components. The heat generated due to these reactions ($HG_{oxidation}$) was calculated with equation (2-22). [24,25]

$$HG_{oxidation} = \sum dH_{i\ oxidation} \cdot m_{i\ \ oxidated} \tag{2-22}$$

$$m_{i\ \ oxidated} = m_{i\ \ before\ allyong} + m_{i\ alloying} - m_{i\ \ alloyed} \tag{2-23}$$

Where i – metal phase component, which is oxidised by alloying,

$dH_{i\ oxidation}$ - enthalpy of the oxidation for the metal phase component i, J/kg.

The enthalpy of the oxidation was calculated based on calculation examples from the practical class “Lab in ferrous metallurgy-processes”. First of all, it is necessary to take into account all the phase transformations (tr1, tr2 etc.) of each oxidised component. [25,34,35]

$$H_T = H_{298} + \int_{298}^{T_{tr1}} c_p dT + \Delta H_{T_{tr-1}} + \int_{T_{tr1}}^{T_{tr-n}} c_p dT + \Delta H_{T_{tr-n}} + \int_{T_{tr-n}}^{T} c_p dT$$
$$where \qquad c_p = a + b \cdot 10^{-3} \cdot T + c \cdot 10^{5} \cdot T^{-2} + d \cdot 10^{-6} \cdot T^{2} \tag{2-24}$$

Where H_{298} – enthalpy of the element in its stable condition (298K). Basically it is equal to 0 J/kg,

c_p– isobar heat capacity, which was calculated, using transformation parameters $(a - d)$

ΔH_{Tr} – enthalpy for the phase transformation

All the transformation parameters and temperatures were taken out from the guidance to physical-chemical calculations for steel electric melting processes performed by department of theory for metallurgical processes of Ural State Technical University. [35]

Enthalpies of metal phase components for oxidation reactions (equations (2-5) - (2-8)) were calculated, using the equation (2-24). Then, enthalpies were multiplied on the corresponding oxidized masses of the metal phase components, as is mentioned in the equation (2-22). The results for the current concept with using of raw magnesite for the slag saturation with MgO (RM-concept) are included in **Table 2-XVI**.

Table 2-XVI: Enthalpies of oxidized elements during alloying and their heat effect [35]

Element	ΔH	$m_{i\ oxidated}$	$HG_{oxidation}$	Sum
	[kJ/kg]	[kg]	[kJ]	
C	-34 100	56	-1 921 028	
Si	-29 400	140	-4 114 667	
Mn	-6 900	61	-418 764	-13 980 250
Al	-32 521	215	-7 006 284	
Fe	-4 990	104	-519 509	

Endothermic effect by current alloying concept is associated with decomposition of carbonates – lime and raw magnesite. The enthalpies of decomposition ($dH_{CO_2}^{carb.}$) of lime and raw magnesite were calculated with "FactSage™ 7.0 Thermochemical Software and Databases" due to the chemical composition of these slag formers **Table 2-I**. After that, these values were multiplied with the corresponding amounts of carbon dioxide in the carbonates respectively like it is mentioned in equation (2-25). Results of this calculation, including summarized endothermic heat effect due to the current alloying concept are included in **Table 2-XVII**. [36]

$$HL_{Decomp.of\ Carb.} = \left(dH_{CO_2}^{lime} \cdot m_{CO_2}^{lime}\right) + \left(dH_{CO_2}^{raw.magn.} \cdot m_{CO_2}^{raw.magn.}\right) \tag{2-25}$$

$$m_{lime}^{CO_2} = \frac{w.\%CO_2}{100} \cdot m_{lime} \tag{2-26}$$

$$m_{raw.mag.}^{CO_2} = \frac{w.\%CO_2}{100} \cdot m_{raw.mag.} \tag{2-27}$$

Table 2-XVII: Enthalpies of decomposition of carbonates during alloying and their heat effect

Carbonate	$dH_{CO_2}^{carb.}$	$m_{carbonate}^{CO_2}$	$HL_{decomposition}$	Sum
	[kJ/kg]	[kg]	[kJ]	
$CaCO_3$	1 780	10.25	18 227.2	456 609.6
$MgCO_3$	1 420	308.72	438 382.4	

Also by alloying during the melting, the metal's state of matter is changing, furthermore material properties are changing too. For example, heat capacity of each melted addition ($Cp_{i\ liquid}$) is not equal to its heat capacity in solid condition ($Cp_{i\ 298}$). Thus, a certain quantity of heat, called "sensitive heat" ($HL_{sesitive}$), has to be taken into account by the estimation of heat losses due to alloying. This amount of heat was calculated with equation (2-28). Some of the materials have a higher melting point ($T_{melting}$) as crude steel. That is why, heat capacities of lime and alumina were taken as an average between solid and liquid state of material. [34]

$$HL_{sensitive} = \sum m_i \cdot \frac{\left(cp_{i\,298} + cp_{i\,TM}\right)}{2} \cdot \left(T_{i\,melting} - 20°C\right) + m_i \cdot cp_{i\,liquid} \cdot \left(T_{steel} - T_{i\,melting}\right) \qquad (2\text{-}28)$$

Table 2-XVIII: Parameters for calculation of sensitive heat losses during alloying [36–40]

Parameters	Unit	FeSi	FeMn	Lime	Raw Magn.	Alumina	Al
$T_{melting}$	[K]	1 316	1 266	2 800	1 053	2 050	933
$Cp_{i\ 298}$	[J/kgK]	530	498	762	859	1 050	1 177
$Cp_{i\ liquid}$		870	950	1 385	1 190	1 888	2 119
$Cp_{i\ average}$		700	724	1 074	1 025	1 469	1 648
$HL_{sesitive}$	[kJ]	564 040	1 355 728	1 324 135	1 074 350	452 932	800 590
Sum		5 631 983					

The enthalpy of fusion of a substance, also known as (latent) heat of melting - HL_{latent}, is the change in its enthalpy resulting from providing heat to a specific quantity of the substance to change its state from a solid to a liquid at constant pressure. It was assumed to take values for each chemical element - j, included in **Table 2-XIX** and then separately multiply them due to its weight content ($w.\%_j$) in the corresponding alloying addition - i (**Table 1-III**) and its mass (**Table 2-XI**). The amount of latent heat per alloying addition - $\Delta H_{latent\ melting\ of\ i}$ is included in **Table 2-XX**. The values were compared with the corresponding results of L. Zhang and F. Oeters in their study [40]. The difference was

assumed as slight, that is why it was decided to perform this calculation in this manner (equation (2-29)) to admit current compositions of corresponding alloying additions.

$$HL_{latent\ of\ i} = \sum m_i \cdot H_{latent\ melting\ of\ i}$$
$$where\ \ H_{latent\ melting\ of\ i} = \sum w.\%_j \cdot m_i \cdot H_{latent\ melting\ of\ j} \quad (2\text{-}29)$$

Table 2-XIX: Latent heat of melting for components, contained in alloying additions [36,39]

Element	Si	Mn	Al	Fe	CaO	MgO	Al_2O_3	CO_2
$\Delta H_{latent\ melting\ of\ i}$, [kJ/kg]	1 926	155	398	272	1 417	1 920	990	184

Table 2-XX: Latent heat of melting for alloying additions, used by current concept

Alloying addition	FeSi	FeMn	Lime	Raw Magn.	Alumina	Al	Coke
HL_{latent}, [kJ]	896 455	370 668	1 134 080	713 019	232 259	96 300	120
Sum	3 442 901						

Consequently, taking into account before the mentioned thermotechnical aspects, it is possible to estimate heat losses caused by alloying due to corresponding concept basing on the following equation (2-30). [36]

$$H_{alloyed\ steel} = H_{crude\ steel} + HG_{oxidation} - HL_{Decomp.of\ Carb.} - HL_{sensitive} - HL_{latent} \quad (2\text{-}30)$$

Temperature of the alloyed steel was calculated with equation (2-21) including some annex. Compared to the crude steel, the heat of alloyed steel is also distributed on generated slag and carbon dioxide gas. Thus, equation (2-31) was used to calculate the temperature of steel after alloying. The heat capacities of slag (cp_{slag}) and CO_2 (cp_{gas}) at 1600°C were assumed as 1230 J/kg·K and 1356 J/kg·K respectively. [36]

$$T_{alloyed\ steel} = \frac{H_{alloyed\ steel}}{m_{alloyed\ steel} \cdot cp_{alloyed\ steel} + m_{slag} \cdot cp_{slag} + m_{gas} \cdot cp_{gas}} \quad (2\text{-}31)$$

Consequently, due to the alloying by tapping temperature of steel was reduced to 34°C and equal to 1567°C. Temperature loses due to the alloying in LF were calculated identically and are equal to 3°C. Thus, based on corresponding concept it is possible to conclude, that the total heat losses due to alloying are equal to 37°C (**Table 2-XXI**).

The alternative alloying concept, with using a doloma instead of raw magnesite for slag saturation with MgO was analysed in the same manner. The total temperature loses by alloying made up 26°C. Thus, it is potentially possible to save 11°C by means of this

substitution. That can be explained by the different alloying addition mix and significantly smaller heat losses, associated with decomposition of carbonates. The comparison of heat and temperature loses due to the alloying concept is included in **Table 2-XXI**, excluding heat generation by oxidation, cause the values are almost equal. [36]

Table 2-XXI: Comparison of heat and temperature losses caused by alloying due to the alloying concept

Heat loss during alloying	Alloying concept		Δ
	with raw magnesite (RM)	with doloma (DL)	
	[MJ]		
sensitive	5 951	5 619	937
due to the decomposition of carbonates	459	22	
latent	3 443	3 275	
Temperature loss during alloying	[°C]		
	37	26	11

2.2.2 Evaluation of heat loses by ladle configurations

Basically, heat is energy transferred as the result of a temperature difference. When the temperature difference exists across the boundary, the Second Law of Thermodynamics indicates the natural flow of energy from hotter body to the colder body. Eventually these two bodies will reach the same temperature and the heat transfer will cease. There are three basic modes of heat transfer:

- conduction,
- convection and
- radiation.

The conduction involves the transfer of heat by the interactions of atoms of a material through which the heat is being transferred. The convection involves the transfer of heat by the mixing and motion of macroscopic portions of a fluid. The radiation is associated with heat transfer by electromagnetic radiation that arises due to the temperature of a body. [41]

In terms of secondary metallurgy, the alloyed steel in the ladle, being a heat supplier, transfers the heat to the refractory contact surface. This transfer, occurred by bulk motion of fluid (liquid steel) is performed by convection. Further, the heat flow inside the ladle walls, including refractory layer and outer steel shell is associated with conduction. And the outer walls of the ladle - side walls, bottom part, as well as liquid steel level, covered by slag transmit the heat to the surrounding air by means of radiation. [42,43]

Hence, to complete the estimation of heat losses as long as the ladle is full of steel, it was necessary to analyse the steel temperature losses under consideration of steel contact time. Due to the configuration of the ladle, heat is proportional transmitted from the steel contact surface through ladle lining and shell to the surrounding air. Also, it was assumed to evaluate the potential to reduce heat losses due to the usage of a cover during two time segments (**WT1** and **WT2**, **Figure 1-8**). To simplify the following calculations, it was assumed to divide the common heat flow from the steel contact surface on three sub flows due to the geometry of the ladle (**Figure 2-3**):

- flow from the bottom part,
- flow from the side wall and
- flow from the slag surface or the outer surface of cover. [44]

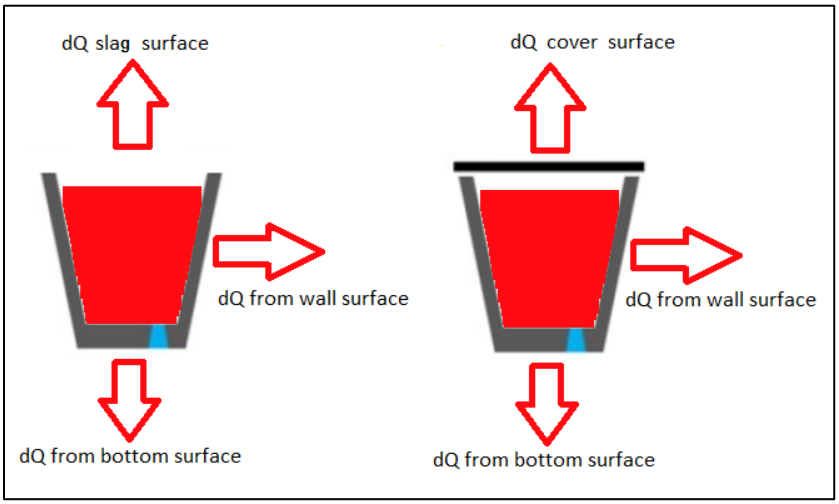

Figure 2-3: Assumed distribution of heat losses due to the ladles configurations [44]

The alternative concept of ladle configuration, mentioned in **Table 1-II**, is a ladle with a cover. It was assumed that, the mentioned cover is manufactured from the materials used in the ladle. The inside surface of cover is manufactured from the same contact refractory type and outer wall of the cover is made of the same steel shell. In this case the heat transmitting consists of three heat transfer types: the radiation from the slag to the inside refractory layer, conductivity inside the cover and heat radiation from the outer steel shell. [44]

The industrial partner provided the drawings of the estimated ladle and confirmed the geometry of the cover. The calculation was based on basics of thermodynamics considering the ladle and surrounding area as a static heat-system, where the energy transmission occurs only due to the temperature difference. Hence in such system all the charged heat is equal to the discharged – equation (2-32). Therefore, the main criterion for the heat balance calculation is the equitability of each sub-flow. That means the calculation can be considered as right only in case, when all partial flows are equal to each other. In other words, the conductivity-heat flow, which brings the heat to the estimated system is equal to the convection and radiation-heat flows, which emit same amount of heat to the surrounding area, like it is mentioned in equation (2-33). [42,44]

$$Q_{charged} - Q_{discharged} = 0 \tag{2-32}$$

$$Q_{conductivity} = Q_{convection} + Q_{radiation} \tag{2-33}$$

Hence, it was necessary, use iteration method to adapt some common values for the contiguous flows. The provided heat-capacity and conductivity values, as well as emissivity coefficients are constant. That is why, the temperature values, used in the calculation have to be balanced considering the equilibration of estimated sub-flows. [44]

The input value for the following calculations was set at temperature of steel after alloying. First of all, to calculate the convection heat flow, it was necessary to take into account the heat transfer coefficient for the heat transmitting from fluid to solid body. For this it is crucial to fix some acceptances, like:

- stationary condition (ladle full of steel),
- free convection,
- the material values (viscosity and convection) were set as the water's by 20°C and
- geometry of ladle is assumed as a perpendicular cylinder.

Next, it was necessary to take into account the dimensionless representation of the heat transfer coefficient - Nusselt number (N_u). This coefficient strongly depends on the thermal boundary condition and flow passage geometry in laminar flow. The Nusselt number is constant for thermally and hydro-dynamically fully developed laminar flow. The determination of the heat transfer coefficient from liquid steel to the refractory layer was done via Nusselt number definition for the perpendicular cylinder: [45,46]

$$N_u = \left(0.852 + 0.387 \cdot \left(Ra \cdot f_1\right)^{\frac{1}{6}}\right)^2 + 0.87 \cdot \frac{h}{d} \tag{2-34}$$

$$f_1 = \frac{1}{\left(1 + \left(\frac{0.492}{Pr}\right)^{\frac{9}{16}}\right)^{\frac{8}{27}}} \tag{2-35}$$

Where Ra – Rayleigh number,

Pr – Prandtl number,

h – high of the cylinder, m

d – diameter of the cylinder, m

The Prandtl number was calculated by dividing of the steel viscosity (ν) value on the coefficient of thermal diffusion (a): [45]

$$Pr = \frac{\nu}{a} = \frac{1.0034 \cdot 10^{-6}}{5 \cdot 10^{-6}} = 0.20068 \tag{2-36}$$

Further, it was necessary to define the Grashof number, which depends on temperature of steel (T_{steel}), temperature of the contact refractory surface ($T_{refractory}$) as well on viscosity and expansion coefficient (β). [45]

$$Gr = \frac{g \cdot h^3 \cdot \beta \cdot \left(T_{steel} - T_{refractory}\right)}{\nu^2} = \frac{9.81 \cdot 4.16^3 \cdot 17.5 \cdot \left(1620 - 1600\right)}{\left(1.0034 \cdot 10^{-6}\right)^2} = 245.5 \cdot 10^{15} \quad (2\text{-}37)$$

Where g – gravitational acceleration, m/s^2,

h – high of the cylinder, m.

Next, it is possible to define the Rayleigh number, via multiplication of Prandtl number and Grashof number: [45]

$$R_a = Gr \cdot Pr = 245.5 \cdot 10^{15} \cdot 0.20068 = 49.26 \cdot 10^{15} \quad (2\text{-}38)$$

Thus, the Nusselt number for the corresponding ladle, assumed as perpendicular cylinder, was calculated via equations (2-34) and (2-35) and is equal to 422.56·10^3 W/m^{2}K. During the negotiations with the industrial partner, based on the internal calculations of steel plant, it was concluded, that this value provides too minor impact. Thus, it was decided to neglect this value (heat transfer coefficient), and assume, that temperature of the contact refractory surface is equal to the steel temperature after alloying – 1564°C by the alloying concept with using of raw magnesite and 1575°C by the alloying concept with using of doloma. [45]

As it was mentioned before, the, heat flow from the contact refractory surface to the steel shell is performed by conductivity, furthermore the conductivity through the multilayer hollow cylinder. Basically, by conductivity flow the heat quantity, transported per time unit through the wall with surface S is determined next equation. [42]

$$Q_{conductivity} = \frac{\lambda}{l} \cdot S \cdot \left(T_1 - T_2\right) \quad (2\text{-}39)$$

Where $Q_{conductivity}$ – heat flow by conductivity, W

λ – heat conductivity of the layer, W/mK

l – thickness of the layer, m

S – area of the conductive surface, m^2

T_1 – temperature of the heat source, °C

T_2 – temperature of the heat receiver, °C

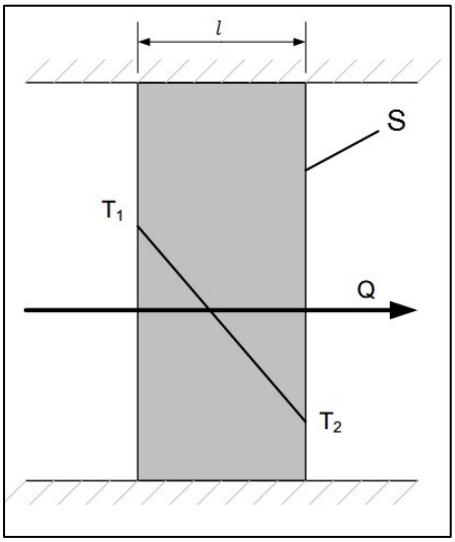

Figure 2-4: Heat flow parameters by conductivity [42]

The conductivity through the multilayer hollow cylinder includes all the same parameters for all corresponding refractory layers. The drawings provided by industrial partner included all the required geometry data, as well as heat conductivity values. [44] Thus, equation (2-40) was used to define first partial heat flow from the side walls:

$$Q_{multilayer\ conductivity} = \frac{2 \cdot \pi \cdot h \cdot \left(T_1 - T_{n+1}\right)}{\left(\frac{1}{\lambda_1} \cdot \ln\frac{r_2}{r_1} + \frac{1}{\lambda_2} \cdot \ln\frac{r_3}{r_2} + \ldots + \frac{1}{\lambda_n} \cdot \ln\frac{r_{n+1}}{r_n}\right)} \tag{2-40}$$

Where h - length of hollow cylinder (height of ladle side wall), m

n - number of the layers,

r - radius from central axe till next layer, m [42]

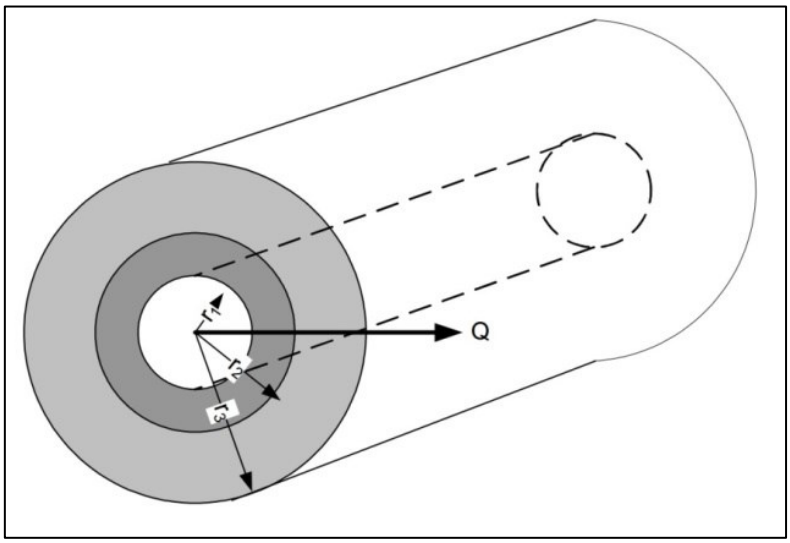

Figure 2-5: Heat flow parameters by conductivity of hollow multilayer cylinder [42]

The heat transmitted from the surface transfers heat to the surrounding area (air) by heat radiation, determined by equation (2-41) with assumption of only one emission coefficient for corresponding surface, which emits the radiation.

$$Q_{radiation} = \sigma \cdot \varepsilon_{shell} \cdot S \cdot \left(T_{shell}^4 - T_{air}^4\right) \tag{2-41}$$

Where σ - the Stefan–Boltzmann constant, W m^{-2} K^{-4}

ε_{shell} - emissivity coefficient of the steel shell. [42]

Thus, to calculate heat flow for the side walls mentioned on the **Figure 2-3**, it is necessary to combine the equation (2-40) with equation (2-41) and to equal these sub flows due to the common temperature of side wall – $T_{side\ wall}$, using the iteration method. Heat flows were balanced by the temperature of side wall equal to 331°C, taking into account steel temperature equal to 1564°C. [42]

$$\begin{cases} Q_{conductivity\ in\ side\ wall} = \dfrac{S_{side\ wall} \times \left(T_{steel} - T_{side\ wall}\right)}{\left(\dfrac{1}{\lambda_1} \times \ln\dfrac{r_2}{r_1} + \dfrac{1}{\lambda_2} \times \ln\dfrac{r_3}{r_2} + \ldots + \dfrac{1}{\lambda_n} \times \ln\dfrac{r_{n+1}}{r_n}\right)} \\ Q_{radiation-side\ wall} = \sigma \times \varepsilon_{shell} \times S_{side\ wall} \times \left(T_{side\ wall}^4 - T_{air}^4\right) \end{cases} \tag{2-42}$$

In the same manner it is possible to calculate heat flow from bottom surface of the ladle, mentioned on the **Figure 2-3**, taking into account the combination of equations (2-40) and (2-41) with the common temperature of the steel shell on the bottom part of the ladle - T_{bottom}. [42]

$$\begin{cases} Q_{conductivity-bottom} = \dfrac{S_{bottom} \cdot \left(T_{steel} - T_{bottom}\right)}{\left(\dfrac{l_1}{\lambda_1} + \dfrac{l_2}{\lambda_2} + \dfrac{l_3}{\lambda_3} + \dfrac{l_4}{\lambda_4}\right)} \\ Q_{radiation-bottom} = \sigma \cdot \varepsilon_{shell} \cdot S_{bottom} \cdot \left(T_{bottom}^4 - T_{air}^4\right) \end{cases} \tag{2-43}$$

Heat flows were balanced by the temperature of bottom equal to 209°C, taking into account steel temperature equal to 1564°C. Such a big difference in temperature between side walls and bottom part of the ladle can be explained by the thicker layer of refractory on

the bottom. Also, these values were approved by the industrial partner, basing on the real operation practice measurements. [45]

The equation (2-41) also suits for the calculation of heat flow from the slag surface (**Figure 2-3**), with an adoption of emissivity coefficient (ε_{slag}) and corresponding square of the slag mirror surface (S_{mirror}). [42]

$$Q_{radiation-slag\ surface} = \sigma \cdot \varepsilon_{slag} \cdot S_{mirror} \cdot \left(T^4_{slag\ surface} - T^4_{air}\right) \quad (2\text{-}44)$$

The temperature and emissivity coefficient of the slag surface were assumed as equal to the temperature and emissivity coefficient of liquid steel to predict the worst case scenario. [45]

Hence, by using previous equations, it is possible to calculate the total heat losses for the ladle caused by its configurations. Next it was crucial to define the total heat losses for the alternative configuration of the ladle – with the usage of the cover (**Figure 2-3**). The only difference from the previous calculations is the heat flow from the slag mirror. This flow is clustered on three sub flows. First is the heat radiation from the slag surface to the inside surface of the cover. Next is performed by the conductivity inside the cover and third is the heat radiation to the surrounding air from the outside surface of the cover. The radiation heat flow between two surfaces, located parallel to each other, can be calculated using next equation: [42]

$$Q_{radiation\ _{s_1-s_1}} = \varepsilon_{s_1} \cdot \sigma \cdot S_{s_1} \cdot \left[\left(\frac{T_{s_1}}{100}\right)^4 - \left(\frac{T_{s_2}}{100}\right)^4\right] \quad (2\text{-}45)$$

Where s_1 – the surface of heat supplier, m

s_2 – the surface of heat receiver, m

It was assumed, that the cover is manufactured from refractory and steel shell. Thus, the combination of equations (2-41) , (2-42) and (2-45) with the common temperatures of inside surface of cover ($T_{cover\ inside}$) and outside surface of cover ($T_{cover\ outside}$) determins the heat flow from the outside surface of cover. [42]

$$\begin{cases} Q_{radiation\ slag-cover} = \varepsilon_{slag} \cdot S_{slag} \cdot \left[\left(\frac{T_{slag}}{100} \right)^4 - \left(\frac{T_{cover\ inside}}{100} \right)^4 \right] \\ Q_{conductivity\ cover} = \frac{S_{cover\ inside} \cdot \left(T_{cover\ inside} - T_{cover\ outside} \right)}{\left(\frac{l_{refractory}}{\lambda_{refractory}} + \frac{l_{steel\ shell}}{\lambda_{steel\ shell}} \right)} \\ Q_{radiation_{cover}} = \sigma \cdot \varepsilon_{steel\ shell} \cdot S_{cover} \cdot \left(T^4_{cover\ surface} - T^4_{air} \right) \end{cases} \quad (2\text{-}46)$$

This system of equation was calculated with temperatures of inside surface of cover equal to 1551°C and outside surface of cover equal to 203°C. These values, which represent theoretical calculation results, were approved by industrial partner as acceptable for the following estimation. [45]

Additionally, it was necessary to estimate heat loses during the time segment, when the ladle is empty after casting (**Figure 1-8**). The equation (2-41) was used to determinate the heat flow radiation from the inside surface of empty ladle. Furthermore, heat radiation from the outside surface, including bottom part of the ladle, was taken into account, and calculated via the same equation. The temperature of inside surface of the ladle after casting was set as experience value – 1300°C. Basing on this value, the system of equations was calculated analogically to previous calculations, equalizing the common temperature of the outside surface of the ladle – T_{bottom} and $T_{side\ wall}$. [42] Hence, the heat loss from the empty ladle was calculated with next equation:

$$\begin{cases} Q_{inside\ surface\ of\ empty\ ladle} = \sigma \cdot \varepsilon_{refractory} \cdot S_{inside\ surface} \cdot \left(T^4_{inside\ surface} - T^4_{air} \right) \\ Q_{outside\ side\ surface\ of\ empty\ ladle} = \sigma \cdot \varepsilon_{steel\ shell} \cdot S_{side\ wall} \cdot \left(T^4_{side\ wall} - T^4_{air} \right) \\ Q_{radiation-bottom} = \sigma \cdot \varepsilon_{steel\ shell} \cdot S_{bottom} \cdot \left(T^4_{bottom} - T^4_{air} \right) \end{cases} \quad (2\text{-}47)$$

All the mentioned systems of equations were correlated due to theirs common temperature parameters using the method of iterations. The calculated values were respectively summarized due to the corresponding configuration of the ladle – with or without cover (**Figure 2-3**). For the case with “no cover” there are three sources (flows) of heat losses: from the slag surface, side walls and the bottom of the ladle (equation (2-48)). For the case with “with cover” there are other three sources (flows) of heat losses: from the cover outer surface, side walls and the bottom of the ladle (equation (2-49)). Thus, it is possible to conclude the results of the heat losses calculation due to the ladle’s configurations in **Table 2-XXII**. All the results are provided in kW, what is equal to the kJ/s.

$$HL_{no\ cover} = \left(Q_{slag} + Q_{side\ walls} + Q_{bottom}\right) \quad (2\text{-}48)$$

$$HL_{with\ cover} = \left(Q_{cover} + Q_{side\ walls} + Q_{bottom}\right) \quad (2\text{-}49)$$

Table 2-XXII: Heat losses due to the ladle's configurations

Configuration of ladle and sources of heat losses		HL (heat losses)	Sum	Δ
		[kJ/s]=[kW]		
no cover	slag mirror	1 476	1 919	1 429
	side walls	421		
	bottom	22		
with cover	cover	46	490	
	side walls	421		
	bottom	22		
empty ladle	refractory surface	2 062	2 155	-
	side walls	78		
	bottom	15		

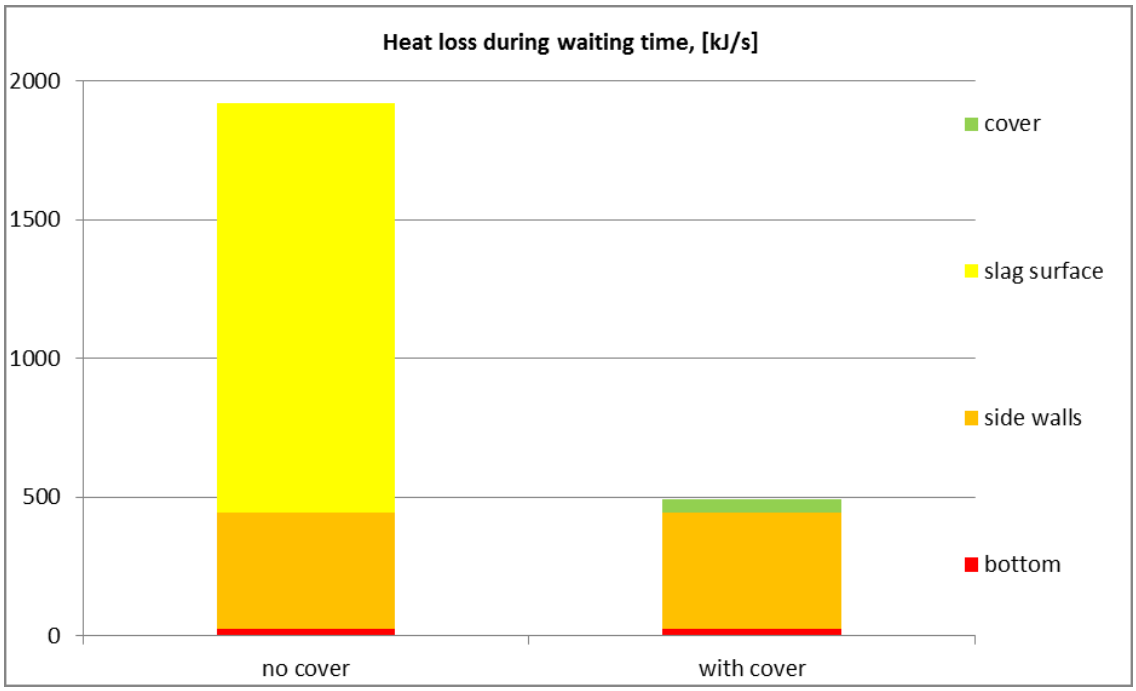

Figure 2-6 Comparison of heat losses per assumed geometry part for two estimated lining configurations – with and without cover

2.2.3 Definition of the total heat and temperature losses per one heat

For the following estimation, it was necessary to adapt previously calculated values of heat losses, caused by the ladle's configuration, considering the schedule of corresponding production route and logistic assumptions mentioned before (**Figure 1-8**). Thus, to define the heat losses due to the ladle's configuration per one heat ($HL_{per\ heat}$), each calculated sum of the heat loses, included in **Table 2-XXII** was respectively multiplied by the duration of the corresponding waiting time segments - WT1, WT2 and WT3 (**Figure 1-8**). Furthermore, each sum was multiplied by 60 to recalculate the result from kJ/sec unit to kJ/waiting time in minutes.

$$HL_{per\ heat} = HL_{WT1} + HL_{WT2} + HL_{WT3} \tag{2-50}$$

$$HL_{per\ heat} = \left(HL_{no/with-cover} \cdot t_{WT1} + HL_{no/with-cover} \cdot t_{WT2} + HL_{empty} \cdot t_{WT3} \right) \cdot 60 \tag{2-51}$$

Where $t_{WT1},\ t_{WT2}\ and\ t_{WT3}$ – duration of waiting time segments (**Figure 1-8**), min

Then, the sum of heat losses per heat, caused by the ladle's configuration, from equation is necessary to divide the preliminary amount of heat, regarding the mass of steel after alloying ($m_{alloyed\ steel}$) and heat capacity of the steel (cp_{steel}) and slag (cp_{slag}), to define the steel temperature losses ($dT_{per\ heat}$), regarding to the logistic assumption and ladle's configuration, mentioned in the **Figure 1-8**.

$$dT_{per\ heat} = \frac{HL_{per\ heat}}{\left(m_{alloyed\ steel} \cdot cp_{steel} \right) + \left(m_{slag} \cdot cp_{slag} \right)} \tag{2-52}$$

Table 2-XXIII: Temperature losses per waiting time segment caused by ladle's configurations

$dT_{per\ heat}$, [°C]				
Logistic assumption	"Good" logistic t_{wt1}=20, t_{wt2}=15, t_{wt3}=40 min		"Bad" logistic t_{wt1}=90, t_{wt2}=30, t_{wt3}=40 min	
Ladle's configuration	no cover	with cover	no cover	with cover
WT1 – before treatment	16	3	70	14
WT2 – after treatment	12	3	22	6
WT3 – after casting	39			
Sum	67	45	131	59
Δ (cover saves)	22		72	

The next step to continue the estimation of the temperature loses (TL_{total}) per one heat was the definition of losses between waiting time segments. They are: temperature losses during tapping (TL_{Tap}), treatment ($TL_{LF-Treatment}$), and casting (TL_{Cast}). Some acceptances are required for these production steps, because they are not static. During the negotiation with the industrial partner it was assumed, to define temperature losses by tapping and casting in the same way as for the static condition, with a half full ladle. Hence, the same equations for the ladle without cover (equations (2-42) - (2-44)), were used to define the steel temperature loss. So, by tapping, which continues for 5 minutes, the steel temperature losses are 4°C. The losses for the casting of ladle on CCM were assumed analogically. However, as mentioned before, the casting is always performed by using a cover on the corresponding steel plant. That means, using the same equations mentioned before for the ladle with cover (equations (2-42),(2-43) and (2-46)) the temperature losses of half-filled ladle with cover make 7°C in 50 minutes.

In addition it was necessary to define the heat losses during the LF ($TL_{LF-Treatment}$) to complete the full list of temperature losses per one heat. The LF-treatment starts with synchronous heating and purging which heats the steel by 4°C per minute ($Heating\ rate$). After the required temperature has been achieved treatment is continued only with purging, which associated with the reducing of steel temperature by 1.5°C per minute ($Cooling\ rate$). The corresponding steel plant the duration of LF-treatment ($t_{LF-treatment}$) was set for 40 min. This means, the duration of heating also depends on the amount of temperature losses during LF-Treatment ($TL_{LF-Treatment}$), which was calculated using the next equations: [47]

$$TL_{LF-Treatment} = (t_{LF-treatment} - t_{heating}) \cdot Cooling\,rate$$

$$where \qquad t_{heating} = \frac{T_{to\ compensate}}{Heating\,rate} \tag{2-53}$$

The temperature to compensate ($T_{to\ compensate}$) was calculated via equation (2-54), taking into account the tapping temperature equal to 1640°C ($T_{Tapping}$), the total steel temperature losses (TL_{total}) and required casting temperature - 1560°C ($T_{Casting}$). It was necessary to summarize the temperature losses by the end of time segment WT2, including the predicted losses of an empty ladle after casting – WT3, to calculate the total steel temperature losses. It is important to notice, that TL_{cast} are not included in the following equations, because the mentioned required casting temperature - 1560°C is the temperature before the beginning of casting. [47]

$$T_{to\ compensate} = T_{Tapping} - \left(T_{Casting} - TL_{total}\right) \quad (2\text{-}54)$$

$$TL_{total} = TL_{All-Tap} + TL_{WT1} + TL_{LF-Treatment} + TL_{All-LF} + TL_{WT2} + TL_{WT3} \quad (2\text{-}55)$$

Where $TL_{All-Tap}$ – temperature losses, caused by alloying during the tapping,

TL_{WT1} – temperature losses by the end of waiting time between tapping and LF-treatment,

$TL_{LF-treatment}$ – temperature losses by the end of LF-treatment (pure purging),

TL_{All-LF} – temperature losses, caused by alloying in the LF,

TL_{WT2} – temperature losses by the end of waiting time between LF-treatment and CCM-casting,

TL_{WT3} – temperature losses by the end of waiting time after CCM-casting.

Thus, after the estimation of all the temperature losses – due to the alloying and ladle's configurations, it was possible to define. Results of the total steel temperature losses per one heat $(TSTL)$ calculation for current alloying concept with using of raw magnesite (RM-concept), are included in **Table 2-XXIV**, due to corresponding assumption (**Figure 1-8**). [47]

Table 2-XXIV: Temperature losses during the one cycle due to production step and logistic assumption by current alloying concept with using of raw magnesite for slag saturation with MgO [47]

Steel temperature losses due to the:	Abbreviation	Logistic assumption			
		A1	A2	B1	B2
		[°C]			
tapping	TAP	4			
alloying by tapping (**RM**-concept)	ALL TAP	34			
waiting time before LF-treatment	WT1	16	3	70	14
LF-treatment (pure purging)	PURG	36	42	19	38
alloying in LF (**RM**-concept)	ALL LF	3			
waiting time before casting on CCM	WT2	12	3	22	6
casting on CCM	CAST	7			
waiting time after casting on CCM	WT3	39			
Total steel temperature losses $(TSTL)$		**151**	**136**	**198**	**146**
$T_{to\ compensate}$, °C		64	49	111	59
$t_{heating}$, min		16	12	28	15

Hence, it is possible to illustrate the time-temperature chart, based on the calculated values. **Figure 2-7** shows the steel temperature changes, when the steel is in the ladle, respectively to the production schedule. Furthermore, in this figure is illustrated two of four logistic assumptions, mentioned on the **Figure 1-8**, for the current alloying concept with using of raw magnesite (RM-concept):

- good logistic of ladle with no cover – RM-A1 and
- good logistic of ladle with cover – RM-A2.

For the proper visualization, it was decided to show the temperature loss of the waiting time after casting on CCM (WT3) together with losses by tapping (TAP) and alloying by tapping (ALL TAP). So, in **Figure 2-7**, these three items from **Table 2-XXIV** are summarized, and on the production step lines (horizontal lines under time-temperature charts), they marked as EAF TAP. Apart from that, the changing of steel temperature during the LF-treatment was illustrated as a common average gradient, based on temperature values before and after LF-treatment. But, in the production step lines the LF-treatment it is divided on two parts. First part illustrates the synchronous heating with purging (HEAT-PURG), and the second part illustrates the pure purging (PURG). Due to the comparing of these two charts it is obviously clear, that potential of using a cover during the waitng time segments reduces the temperature losses, as well as the heating time during the LF-treatment. Thus, such potential improvement increases the energy efficiency of the secondary metallurgy and reduces indirect CO_2 emissions, associated with the purchasing of electric energy (**Figure 1-2**). [48]

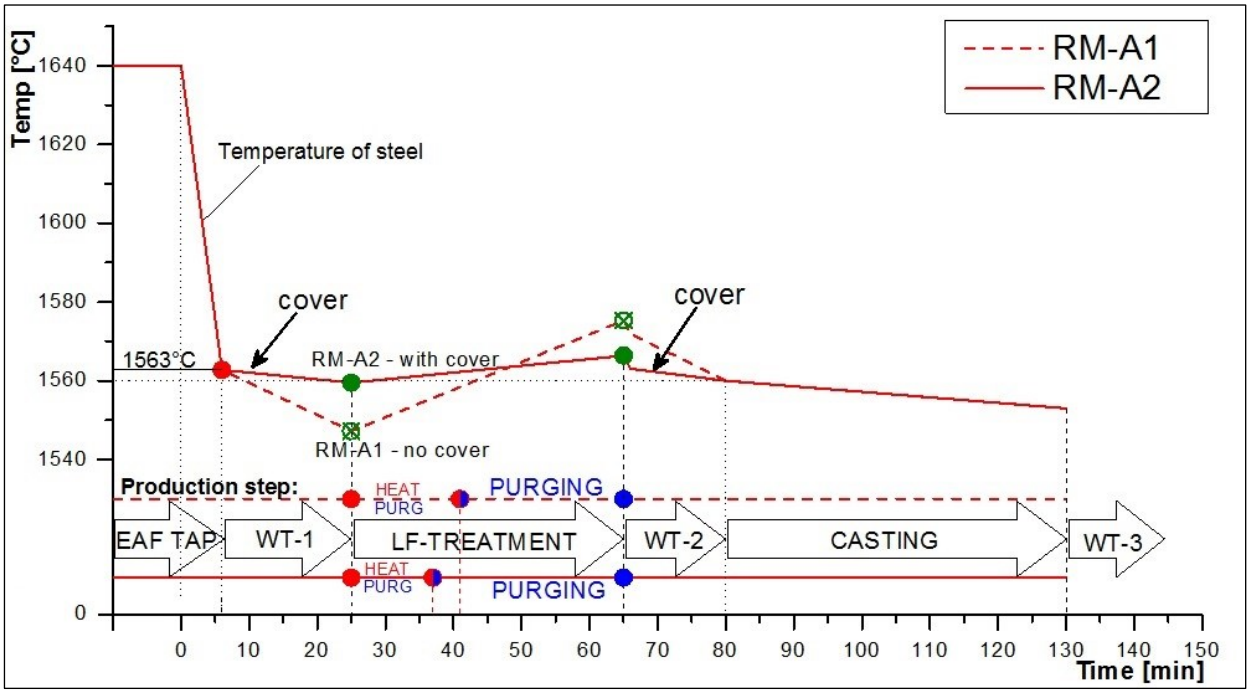

Figure 2-7: Time-temperature charts during one heat for cases "good logistic" RM-A1 (raw magnesite - no cover), RM-A2 (raw magnesite - with cover) due to the corresponding production step [48]

Total steel temperature losses ($TSTL$) for the alternative alloying concept with using of doloma for the slag saturation (DL-concept) were calculated in the same manner. The results for the same logistic assumptions (good logistic of ladle with no cover – DL-A1 and good logistic of ladle with no cover – DL-A1) are included in **Table 2-XXV** and illustrated in the **Figure 2-8**. [48]

Table 2-XXV: Temperature losses during the one cycle due to production step and logistic assumption by alternative alloying concept with using of doloma for slag saturation with MgO

Steel temperature losses due to the:	Abbreviation	Logistic assumption			
		A1	A2	B1	B2
		[°C]			
tapping	TAP	4			
alloying by tapping (**DL**-concept)	ALL TAP	22			
waiting time before LF-treatment	WT1	16	3	71	15
LF-treatment (pure purging)	PURG	39	45	21	41
alloying in LF (**DL**-concept)	ALL LF	3			
waiting time before casting on CCM	WT2	12	3	22	6
casting on CCM	CAST	7			
waiting time after casting on CCM	WT3	39			
Total steel temperature losses $(TSTL)$		143	127	191	138
$T_{to\ compensate}$, °C		56	40	104	51
$t_{heating}$, min		14	10	26	13

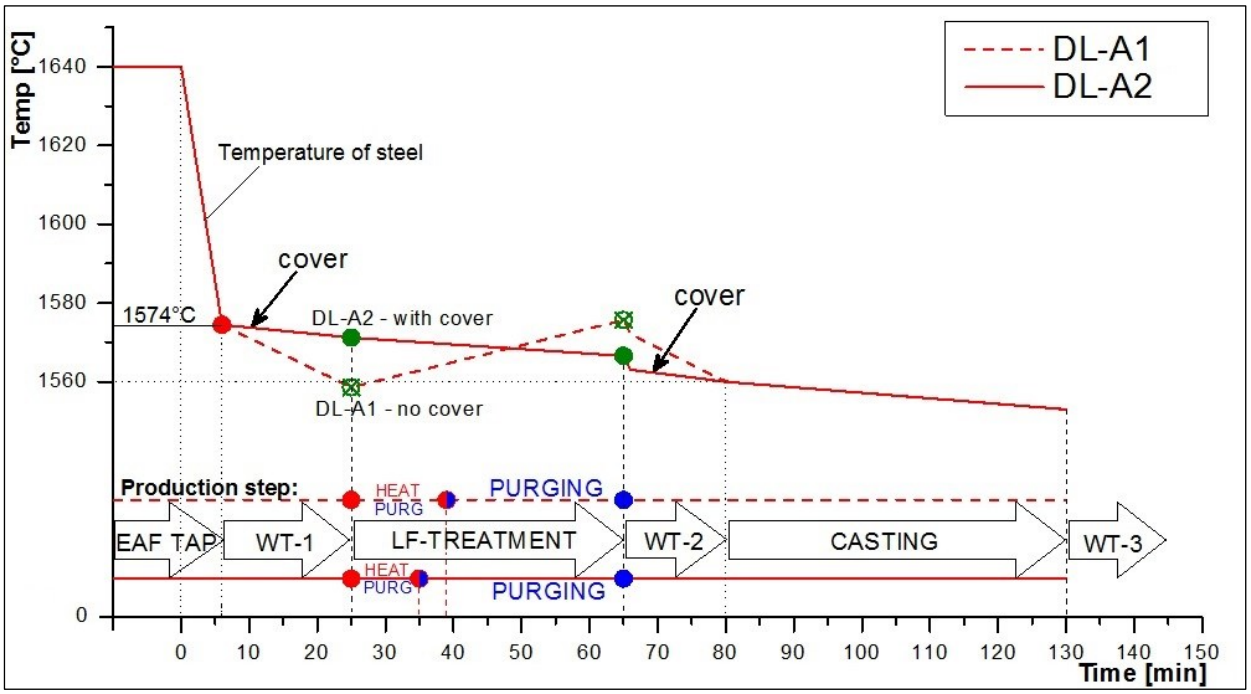

Figure 2-8: Time-temperature charts during one heat for cases “good logistic” DL-A1 (doloma - no cover), DL-A2 (doloma - with cover) due to the corresponding production step [48]

The results for other logistic assumptions, with longer waiting time segments (cases B1 and B2 on the **Figure 1-8**) for both alloying concepts were illustrated together. As mentioned before, the alternative alloying concept with using doloma is associated with less

temperature loss during alloying by tapping. So, in the **Figure 2-9**, this difference is obviously clear – 11°C by EAF-TAP segment. The time-temperature charts of logistic assumptions B1 (bad logistic, no cover, **Figure 1-8**) demonstrate, that temperature of steel drops under the liquidus temperature, even before the end of WT1-segment. Based on the calculation parameters from **Table 2-XVIII**, it is possible to conclude, that amount of heat to preheat the liquid metal and amount of heat to melt the solid metal are not equal (comparable). This means, that these two assumptions **RM-B1** and **DL-B1** (bad logistic, no cover, **Figure 1-8**) may not be involved to the following common estimation. That is why any production lines for these assumptions are not included in the **Figure 2-9**. [48]

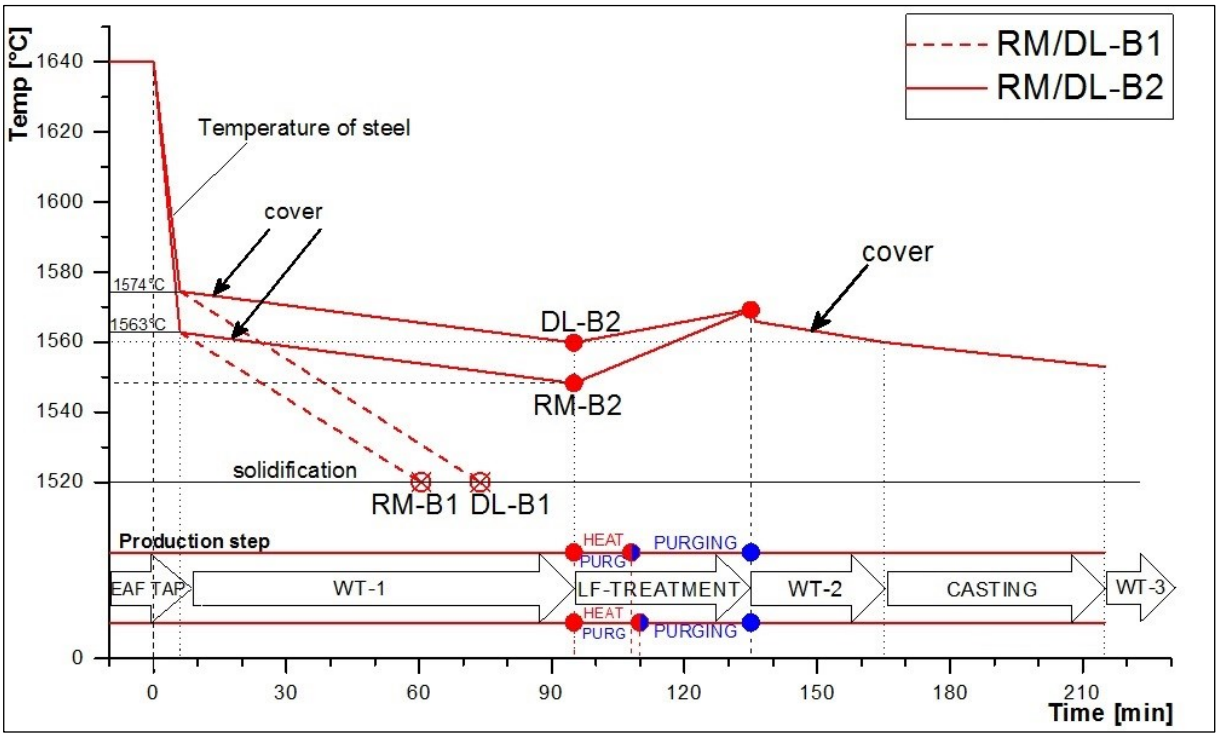

Figure 2-9: Time-temperature charts during one heat for cases “bad logistic” RM-B1 (raw magnesite - no cover), RM-B2 (raw magnesite - with cover), DL-B1 (doloma - no cover) and DL-B2 (doloma - with cover) due to the corresponding production step [48]

All the corresponding results were approved during the series of negotiations with industrial partner. In terms of the theme of this study, it was necessary to complete the estimation of current production route with the definition of energy efficiency. The results of previous calculations showed that heating duration by LF-treatment ranges, due to the logistic assumption. The longer heating requires more electricity to purchase. Furthermore, the higher energy consumption implies more indirect CO_2 emissions (*Scope 2*, **Figure 1-2**) and more direct CO_2 emissions via electrode’s combustion.

2.3 Definition of the energy consumption

First of all, it was necessary to combine the evaluation of the heat losses and amount of required electricity, to define the energy consumption per one heat, due to the logistic assumption (**Figure 1-8**). The amounts of temperature to be compensated ($T_{to\ compensate}$, in **Table 2-XXIV** and **Table 2-XXV**) were respectively multiplied by the total mass of alloyed steel (including the mass of slag) and its heat capacity (cp_{steel}). The unit of resulted amount of heat to purchase during the treatment (Q_{loss}) was assumed in MJ. [49]

$$Q_{loss} = T_{to\ compensate} \cdot \left(m_{steel} + m_{slag} \right) \cdot cp_{steel} \tag{2-56}$$

Next, it was necessary to convert the calculated amount of required heat, to the amount of required electricity per t_{ls} ($special\ Q_{loss}$). Basically, one watt hour is equal to 3600 Joules, that means that 1 kilowatt hour (kWh) is equal to $3.6 \cdot 10^6$ Joules. Thus, taking into account the amount of alloyed steel, it is possible to calculate the amount of required electricity per t_{ls} in kWh/t_{ls} unit. The calculated results for both of alloying concepts are provided below in **Table 2-XXVI** due to the logistic assumption. [49]

$$special\, Q_{loss} = \frac{Q_{loss}}{3.6 \cdot 10^6 \cdot m_{steel}} \tag{2-57}$$

Table 2-XXVI: Energy consumption for one production cycle due to logistic assumption, ladles configuration and alloying concept (RM - concept with using raw magnesite, DL – concept with using doloma)

Assumption	Abb.	**RM**-concept	**DL**-concept	Substitution of RM to DL
		[kWh/t_{ls}]		
"good" logistic, no cover	A1	15.15	13.26	~2.0
"good" logistic, with cover	A2	11.50	9.52	
"poor" logistic, with cover	B2	13.92	11.96	
Comparison of the assumptions to evaluate the potential electricity savings				
Logistic improvement	B2-A2	~2.43		
Using of cover	A1-A2	~3.70		

The comparison of the values, included in **Table 2-XXVI**, are performed to evaluate the potential savings of energy by means of different improvements. For example, due to the potential substitution of raw magnesite by doloma, it is possible to reduce the energy consumption of LF-treatment on 2 kWh/t_{ls}. Apart from this, the difference between assumptions B2 and A2 ("good" and "bad" logistic; with cover, **Figure 1-8**) shows the potential energy savings, due to the possible waiting time segments duration reduction ("Logistic improvement", **Table 2-XXVI**). In the same manner, the difference between assumptions A1 and A2 (no cover and with cover; "good" and "poor" logistic, **Figure 1-8**) shows the potential energy savings due to the using of cover during these waiting time segments ("Using of cover", **Table 2-XXVI**).

3 Definition and calculation of the CO_2 emission

After the settling of current and alternative alloying concepts, including the corresponding temperature losses and energy consumption, due to the logistic assumption, it was necessary to define the related CO_2 emissions. Coming back to the classification of the carbon dioxide emissions noticed in the **Figure 1-2**, it was decided to correlate three *Scopes* of emissions and emission sources due to the estimated production step.

As it was mentioned before, the first production step of the corresponding route is EAF-tapping. The first alloying of the crude steel is also performed during tapping. Thus, decomposition of charged carbonates, unrecovered part of carbon as well carbon dioxide, coming with other alloying agents, assemble the direct emission of CO_2. The amount of these emissions were calculated with equation (2-16). Apart from that, the purchasing of required alloying additions are associated with indirect emissions from *Scope 3* (**Figure 1-2**).

The next production step was assumed as waiting time before LF-treatment (WT1, **Figure 1-8**). Different variations of logistic assumptions and ladle's configurations (cover, no cover) were estimated and recalculated to correlated heating duration and corresponding energy consumption. Thus, from the point of view of GHG emissions, the heating process during the LF-treatment is associated with electrode combustion, which provides direct emission of CO_2. Also, the purchasing of electricity during this time segment is a source of indirect emissions from *Scope 2* (**Figure 1-2**). Apart from that, it is necessary to take into account the purchasing of refinement gas (Argon) and its indirect emission from *Scope* 3.

The second alloying is performed after the LF-treatment. The previous settling of alloying concepts (**Table 2-XI** and **Table 2-XIII**) showed that the small amount of carbon is needed to

be added to the steel after LF-treatment. So, due to not fully recovering, it will provide direct emission. Also, indirect emissions, due to the purchasing of other alloying additions have to be taken into account. [50]

The service of empty ladle after casting is the next and the last step of estimated production route, which is associated with carbon dioxide emissions. It was assumed, that the lifetime of the ladle's refractory lining is 110 heats and no hot repair is performed during this period. Thus, after each 110 heats, the ladle has to be fully relined. So, the experience value of refractory consumption (1.2 kg/t_{ls}) has to be estimated according to the corresponding indirect emission coefficient for *Scope 3*. After that the new refractory has to be preheated by gas burners, this process called ladle's preheating treatment. It is obviously clear, that the combustion of natural gas required for this preheating provides direct emission of carbon dioxide. [50]

The classification of above mentioned emission sources due to the production step is included in **Table 3-I**. It was assumed to calculate all the estimating values in kg_{CO2}/t_{ls} unit. The refractory consumption occurs during the whole production cycle, but for the simplification, it was decided to associate the corresponding emissions from *Scope 3* only during service.

Table 3-I: the classification principle of corresponding emission items due to the production step [50]

Production step	CO_2 emission per one heat by corresponding production route		
	Direct	Indirect	
	Scope 1	*Scope 2*	*Scope 3*
Tapping	unrecovered carbon, slag former's decomposition	-	purchasing of alloying additions
Heating	combustion of electrodes	purchasing of electricity	-
Purging	-	-	purchasing of argon
Alloying in LF	unrecovered carbon	-	purchasing of alloying additions
Service	natural gas combustion during preheating treatment	-	refractory consumption

The direct emissions were partly calculated by the settling of alloying concepts, the results are provided in **Table 2-XV**. Thus, it was necessary to calculate the combustion of electrodes during the heating by LF-treatment and combustion products by preheating treatment. The purchasing of electricity has to be evaluated basing on different logistic assumption and corresponding emission coefficient for *Scope 2*. According to the indirect emissions from *Scope 3*, it was necessary to estimate each certain purchased material due to its amount and emission coefficient.

3.1 Estimation of direct emissions

The values of the direct emission due to the alloying were already considered by developing of two alloying concepts (**Table 2-XV**). Thus, the direct emission by current alloying concept with the using of raw magnesite (RM-concept) is associated with 3.06 kg_{CO2}/t_{ls}, and by alternative concept with using doloma (DL-concept) with 1.27 kg_{CO2}/t_{ls}.

While the steel is preheating during the LF-treatment by means of electric arc, the electrode is burning off. During the negotiations, it was assumed to take into the account experience value of electrode consumption – 6 g of electrode per kWh of purchased electricity, required for the heating. It was assumed to predict the "worst case" scenario - the full oxidation of pure carbon (100 w.% C) via next chemical reaction: [50]

$$[C]+\{O_2\}\rightarrow\{CO_2\} \tag{3-1}$$

Thus, to calculate the mass of generated carbon dioxide, it was necessary to multiply the consumption rate (0,006 kg per kWh) with corresponding required electricity per t_{ls} ($special\ Q_{loss}$, calculated with equation) and molar mass ratio (carbon oxide to carbon). The calculated mass was divided on the heat size to recalculate the value to kg_{CO2}/t_{ls} unit: [50]

$$\frac{m_{CO_2}}{m_{heat}}=\left(consumption\ rate\cdot Q_{special}\cdot\frac{M_{CO_2}}{M_C}\right)\div m_{heat} \tag{3-2}$$

Hence, taking into account the average heating duration for three estimated logistic assumptions (15 minutes for RM-concept and 13 minutes for DL-concept from **Table 2-XXIV** and **Table 2-XXV**), combustion of electrode provides 0.33 kg_{CO2}/t_{ls} and 0.28 kg_{CO2}/t_{ls} respectively.

The ladle preheating treatment was assumed as one of the most important sources of direct emissions in the beginning of project. The calculation of natural gas combustion was

also performed based on "worst case" parameters. Pure methane (100 w.% CH_4) instead of natural gas was taken, which is supposed to be fully burned to carbon dioxide and water (steam) via next chemical reaction: [50]

$$\{CH_4\} + 2\{O_2\} \rightarrow \{CO_2\} + 2\{H_2O\} \tag{3-3}$$

The usual duration of preheating treatment to the corresponding production route is 8 hours, with the flowrate of natural gas equal to 350 Nm^3/hour. The mass of 1 Nm^3 of methane is 0.717 kg. [51] That means, 2007.6 kg of methane is required for 8 hours of preheating the ladle. Taking into account, that molar quantities of methane and carbon dioxide are equal, it is possible to calculate the mass of generated CO_2.

$$\frac{m_{CH_4}}{M_{CH_4}} = \frac{m_{CO_2}}{M_{CO_2}} \quad ; \quad \frac{m_{CO_2}}{m_{heat}} = \left(\frac{m_{CH_4} \cdot M_{CO_2}}{M_{CH_4}} \right) \div m_{heat} \tag{3-4}$$

Thus, 8 hours of preheating a ladle produce 5521 kg of CO_2, what is equal to 0.29 kg_{CO2}/t_{ls}. In **Table 1-II** the prolonged duration of ladle preheating treatment up to 10 hours provides 6211 kg of CO_2, what is equal to 0.33 kg_{CO2}/t_{ls}. So, each additional hour of preheating causes 0.02 kg_{CO2}/t_{ls} by current production parameters.

Hence, summing up all the estimated sources of direct emissions by current production route, it is possible to conclude the calculated amounts of CO_2 emissions in **Table 3-II**. The values for potential prolonged duration of ladle preheating treatment up to 10 hours are noticed in brackets. [50]

Table 3-II: Estimated sources of direct emissions during the production cycle due to the alloying concept (RM - concept with using raw magnesite, DL – concept with using doloma) [50]

Production step	Direct Emission of CO_2 per one production cycle, [kg CO_2/t_{ls}]	
	RM-concept	DL-concept
alloying by tapping	3.01	1.23
heating by LF-treatment	0.33	0.29
alloying in LF	0.05	0.04
ladle preheating treatment - 8 h (10h)	0.29 (0.33)	
Sum	3.65 (3.70)	1.82 (1.87)

It is obviously clear, that the main source of direct emissions at the secondary metallurgy is the chemical processes during alloying by tapping. Furthermore, the saturation of slag by MgO and implied decomposition of carbonates seems to be the key factor to reduce direct emissions. Taking into account corresponding production parameters, potential substitution of raw magnesite on doloma, it can reduce the total direct CO_2 emissions more than twice - from 3.65 to 1.82 kg CO_2/t_{ls}.

According to the real operation practice during the secondary metallurgy, it was decided to estimate the prolongation of preheating duration based on the quantity of required ladle preheating treatments per year by annual steel production 1 Mio tones. Taking into account the corresponding heat size, it is possible to calculate how many heats are required to achieve the 1 Mio tones in one year – 5882, **Table 3-III**. Further, based on the assumed refractory lifetime – new lining is performed once in 110 heats - it is possible to define the corresponding annual number of ladle preheating treatments – 53, **Table 3-III**. Assuming the prolongation of preheating treatment up to 9 and 10 hours and multiplying these values on annual number of preheatings, is possible to conclude, that each regular additional hour of ladle preheating treatment causes 36.6 tCO_2/year. The results of this calculation are included in **Table 3-III**.

Table 3-III: Influence of the ladle preheating treatment duration on the amount of direct CO_2 emissions per year under the consideration of production of 1 mio tons of steel by corresponding production parameters

Duration of ladle preheating treatment, [h]	Annual data by annual steel production 1 Mio tones		
	Number of heats	Number of preheatings	direct CO_2, [t]
8	5882	53	292.6
9			329.2
10			365.8
Annual emission, caused by regular additional hour of ladle preheating treatment			36.6

3.2 Estimation of indirect emissions

3.2.1 Emissions from Scope 2

The amount of indirect CO_2 emissions from *Scope 2* are equivalent to the amount of purchased of electricity. The results of the calculation of specific electricity consumption (per t_{ls}) are included in **Table 2-XXVI**. Based on these values, it was necessary to estimate the associated indirect emission amount. The calculation of emissions from electricity in majority of countries based on factors, published by the International Energy Agency (IEA 2010). But these factors include emissions from heat generation, which may skew the factor upwards and downwards. The British company "Ecometrica", which bring together sustainability, environment and business management with geospatial intelligence, has specified a table of CO_2 emissions coefficients. The coefficients in this spreadsheet are based on the amount of emissions, divided by total kWh of electricity consumed. Estimation of these factors account the calculation of the total emissions from the generation of electricity within a country and dividing this value by the total amount of electricity, produced by the country. [52] [53]

Table 3-IV: Emission coefficients for Scope 2 [52]

Country	Electricity-specific factors, [kg_{CO2}/kWh]
Austria	0.1768
Brazil	0.0926
China	0.9746
Germany	0.6722
IEA Europe*	0.4537
IEA North America	0.4994
IEA Total	0.4889
India	1.3332
Korea	0.5044
Russian Federation	0.5132
United Kingdom	0.5085
United States	0.5471
*IEA – International Energy Agency	

Thus, due to the corresponding emission coefficient, the amount of indirect emission can widely range. It was assumed to take into account the IEA Europe coefficient – 0.4537 kg_{CO2}/kWh and multiplied it by the calculated values from **Table 2-XXVI**. [52]

So, based on the calculated values of energy consumption due to the logistic assumption, included in **Table 2-XXVI**, it is possible to estimate the amount of corresponding emissions from *Scope 2*. For that, values from **Table 2-XXVI** were multiplied by coefficient – 0.4537 kg_{CO2}/kWh. Apart from such recalculation, the analogical comparisons of some assumptions are noted in **Table 3-V**.

Table 3-V: Amounts of CO_2 emission from the *Scope 2*, due to the logistic assumption and alloying concept and influence of estimated improvements on CO_2 emission amount (*Scope 2*) per one heat

Assumption	Abb.	**RM**-concept	**DL**-concept	Substitution of RM to DL
		[$kgCO_2/t_{ls}$]		
"good" logistic, no cover	A1	6.87	6.02	~0.88
"good" logistic, with cover	A2	5.22	4.32	
"poor" logistic, with cover	B2	6.32	5.42	
Comparison of the assumptions to evaluate the potential CO_2 savings (*Scope 2*)				
Logistic improvement	B2-A2	1.10		
Using a cover	A1-A2	~1.68		

It is obviously clear, that potential substitution of slag generator provides the smallest emission reduction input, considering the indirect CO_2 emissions from *Scope 2*. Apart from that, such substitution as well using of cover during waiting time segments require additional financial investments compared to the potential improvement of the ladle's logistic. Hence, the most significant role of indirect emissions reduction from *Scope 2* is the use of the cover. But still, such improvement causes the external emissions, associated with manufacturing and preheating of such covers.

3.2.2 Emissions from Scope 3

Scope 3 includes indirect emissions, associated with purchasing of materials, used in the production route. Taking into account the items from **Table 3-I**, it possible to divide all the supply materials into three 3 groups: alloying additions, gases and refractory materials. The amount of each alloying addition was estimated due to the alloying concept by means of the special value in kg per t_{ls} unit in **Table 2-XI** and **Table 2-XIII**. Thus, to evaluate the indirect emission from *Scope 3*, it was necessary to estimate the production of each certain item, like alloying addition, gas and refractory, from the point of view of the emission input.

To produce the ferroalloy, it is necessary to mix and heat the raw ore, carbon materials and slag forming material for following reduction and smelting. The carbonaceous reductants as well charcoal and wood are usually used as carbon source. Reduction process results in significant carbon dioxide emissions. Based on calculating methodology and the values from the article prepared by SINTEF Materials and Chemistry, a research institute for the twelfth International Ferroalloys Congress in Helsinki on 2010, next emission coefficients for FeSi and FeMn were taken for following estimation: 3.8 tCO_2/tonne of FeSi and 1.45 tCO_2/tonne of FeMn. [54]

As for aluminium, basically there are two production modes: primary and secondary. Primary aluminium production is conducted in basically two process steps, namely the production of the intermediate product aluminium oxide or alumina (Al_2O_3) in the Bayer chemical process and the following conversion to aluminium by electrolysis. In secondary aluminium production new and old aluminium scrap are converted into new ingots, which are widely used as deoxidiser for the steel industry or delivered as molten metal. The most significant process emission in the primary aluminium production is the consumption of prebaked carbon anodes during the chemical conversion aluminium oxide to aluminium metal. Due to the type of technology process – Prebake or Soderberg, processes are associated with 1.6 tCO_2/tonne of Al and 1.7 tCO_2/tonne respectively. The secondary production, which basically includes melting and refining, is associated with 0.22 tCO_2/tonne of Al. Usually secondary aluminium is used at the secondary metallurgy, that is why it was assumed to consider corresponding emission coefficient 0.22 tCO_2/tonne of Al of purchased aluminium. -[55]

The emission coefficient for production of alumina, used for slag forming, was taken out of the methodology developed by ECOFYS Company by order of the European Commission in 2009. Thus, production of alumina is associated with 0.39 tCO_2/tonne of product. [56]

The world steel association collected and reported the CO_2 emission data on a site-by-site basis to give overall emission intensity, irrespective of final products that are being made. Thus, next emission factors were defined and agreed by a world steel panel of experts: 0.95 tCO_2/tonne of burnt lime and 1.1 tCO_2/tonne of burnt dolomite. As well the emission coefficient for the purchase of coke was taken from the same user guide – 0.22 tCO_2/tonne of product. The emission coefficient for production of raw magnesite was settled during the consultation with Prof. Schenk. [53]

Each mentioned emission coefficient was multiplied with corresponding amount of alloying addition due to the alloying concept (**Table 2-XI** and **Table 2-XIII**). Thus the summarised emission inputs of alloying process for both of the alloying concepts, considering the corresponding emission coefficient for alloying addition are included in **Table 3-VI** and **Table 3-VII**.

Table 3-VI: Emission coefficients and amount of CO_2 emission from Scope 3 per addition for the alloying concept with raw magnesite (RM-concept) [53–56]

RM-Alloying concept		Emission input of alloying (*Scope 3*)						
		FeSi [54]	FeMn [54]	Lime [53]	R.Magn.	Alumina [56]	Al [56]	C [53]
Emission coefficient	[$kgCO_2$/kg]	3.80	1.45	0.95	0.02	0.39	0.22	0,22
Addition by tapping	[kg/t_{ls}]	3.68	8.82	4.71	4.00	3.47	0.88	0.32
Addition in LF		0.29	0.26	-	-	-	-	0.19
Emission per addition	[$kgCO_2/t_{ls}$]	15.08	13.17	4.47	0.08	1.35	0.19	0.07
Sum		**34.45**						

Table 3-VII: Emission coefficients and amount of CO_2 emission from Scope 3 per addition for the alloying concept with doloma (DL-concept) [53–56]

DL-Alloying concept		Emission input of alloying (*Scope 3*)						
		FeSi [54]	FeMn [54]	Lime [53]	Doloma [53]	Alumina [56]	Al [56]	C [53]
Emission coefficient	[$kgCO_2$/kg]	3.80	1.45	0.95	1.10	0.39	0.22	0.22
Addition by tapping	[kg/t_{ls}]	3.69	8.82	2.44	4.40	3.44	0.88	0.31
Addition in LF		0.44	0.35	-	-	-	-	0.15
Emission per addition	[$kgCO_2/t_{ls}$]	15.67	13.30	2.32	5.67	1.34	0.19	0.10
Sum		**38.60**						

It is clear, that the alternative alloying concept provides more indirect emissions from *Scope 3*. That can be explained by burning process, used in doloma production. But the

difference of indirect emission input (*Scope 3*) between these concepts is about 9% relative. In terms of the current evaluation, addition to alloying input it was necessary to estimate the indirect emissions caused by purchasing other supply materials. Hence, during the LF-treatment, which continues 40 min, steel is purged with argon. The flowrate of Argon was taken out of the technical description to corresponding LF and equal to 500 Nm^3/min. Thus, for each production cycle it is necessary to purchase 2000 Nm^3 of Argon. The emission coefficient was provided from user guide to CO_2 emission data collection developed by Worldsteel association. Thus, taking into account that, production of 1kNm^3 of Argon implies 0.103 tCO_2/tonne, each LF-treatment cause 0.012 kgCO_2/t_{ls}. [53]

The last item of estimated sources indirect emission, associated with purchasing of supply materials is refractory. The refractory consumption by current production route is 1.2 kg/t_{ls}. In 2013 the European Refractories Producers' Federation developed a carbon footprint report, where the emission coefficient for basic fired shaped refractory is equal 0.478 tCO_2/tonne. Thus, during one production cycle 0.57 kgCO_2/t_{ls} is provided by purchase of refractories. [57]

Taking into account all the mentioned values and items, excluding other potential sources of indirect emissions, like waste of disposal, it is possible to summarise the results in **Table 3-VIII**. It is obviously clear that the part of indirect emissions is associated with the purchase of alloying additions. The potential substitution of doloma in the current raw magnesite would increase the indirect CO_2 emissions, due to the higher emission coefficient and other alloying addition mix (**Table 3-VII**).

Table 3-VIII: Comparison of the CO_2 emission amount from Scope 3 due to the production step for the current (RM-concept) and optional (DL-concept) alloying concepts

Production step	Estimated item	Amount in kgCO_2/t_{ls}		Δ
		RM-concept	DL-concept	
Tapping	purchasing of alloying additions by RM-concept (DL-concept)	32.94	36.40	-3.46
Purging	purchasing of argon	0.012		-
Alloying in LF	purchasing of alloying additions by RM-concept (DL-concept)	1.52	2.20	-0.68
Service after casting	refractory consumption	0.57		-
	Sum	35.04	39.18	-4.14

3.3 Distribution of emissions due to the Scope

All the previously mentioned emission input values were summarised due to the production step and alloying concept. Thus, **Table 3-IX** includes the total CO_2 emission per one production cycle due to the *Scope* for alloying concepts with raw magnesite (RM-concept) and doloma (DL-concept). The value of electricity consumption, furthermore the amount of emission from *Scope 2*, were assumed as average value between estimated assumptions from **Table 3-V**.

Table 3-IX: Comparison of the average CO_2 emission amount per one production cycle for the current (RM-concept) and optional (DL-concept) alloying concept

Production step	[$kgCO_2/t_{ls}$]					
	Direct		Indirect			
	Scope 1		*Scope 2*		*Scope 3*	
	RM-concept	**DL**-concept	**RM**-concept	**DL**-concept	**RM**-concept	**DL**-concept
Alloying by tapping	3.01	1.23	-		34.20	37.66
Heating	0.31	0.27	6.14	5.25	-	
Purging	-		-		0.012	
Alloying in LF	0.05	0.04	-		1.52	2.20
Service after casting	0.29		-		0,57	
Sum per Scope	**3.65**	**1.82**	**6.14**	**5.25**	**35.04**	**39.18**
Δ per Scope	1.83		0.89		-4.14	
Sum for **RM**	44.83					
Sum for **DL**	46.25					
Δ	**-1.42**					

The comparison of the amounts of emissions due to the *Scope* obviously shows that biggest part of total CO_2 emissions in secondary metallurgy is associated with *Scope 3*. By current parameters, for both of the alloying concepts they account around 80% of the total amount. Also it is clear that total emission input of an alternative concept is bigger than the current. At the same time potential substitution of alloying concept reduces twice. But still the direct emissions at the secondary metallurgy are associated for only 5% of the total amount.

The emissions from *Scope 2* by corresponding logistics count for only 15% of the total amount. Of course, potentially this part can widely range according to emission coefficients (**Table 3-IV**). Calculated values from **Table 3-IX** are illustrated on the **Figure 3-1**.

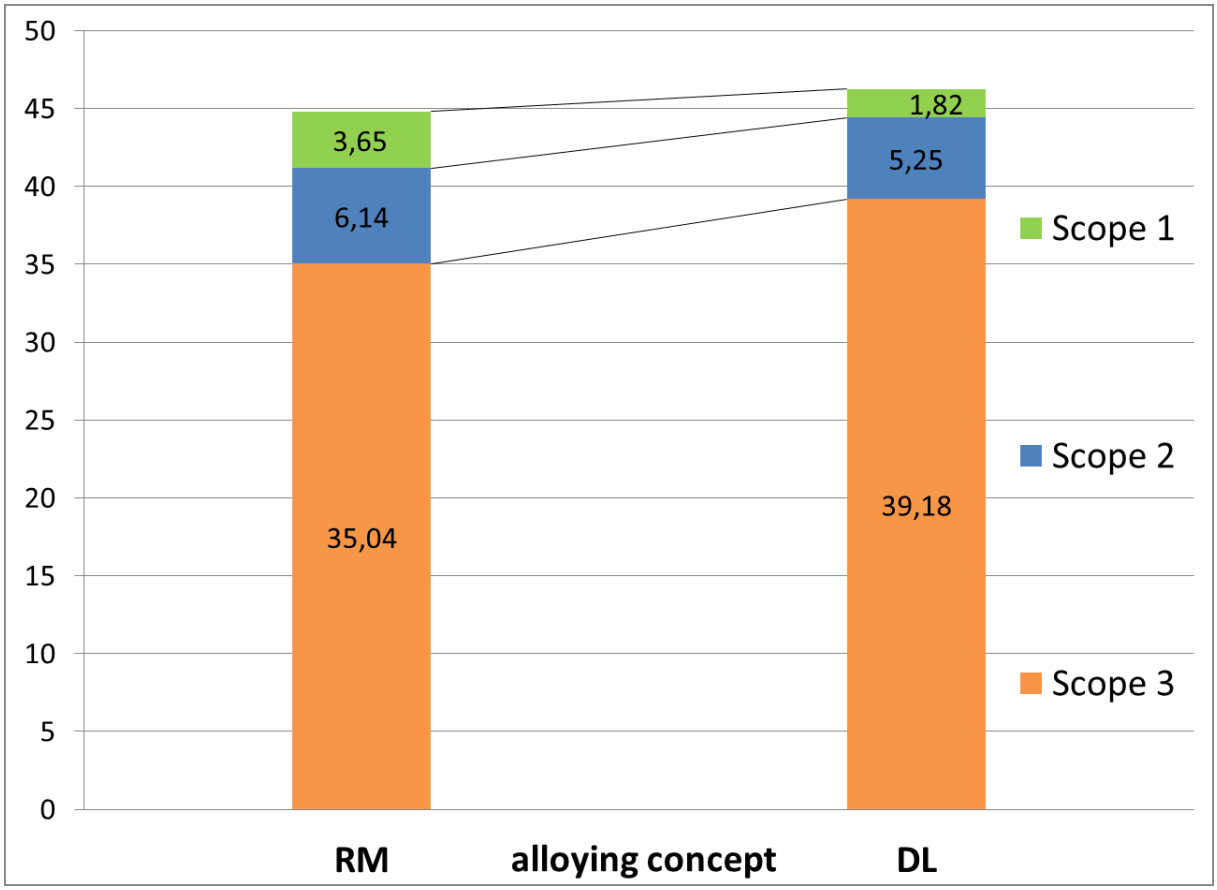

Figure 3-1: Emission of CO_2 per one production cycle due to the alloying concept in $kgCO_2/t_{ls}$

The CO_2 emission distribution due to the estimated logistic assumption, mentioned in the **Figure 1-8** was calculated and respectively added on previous **Figure 2-7**, **Figure 2-8** and **Figure 2-9**. Hence, all previously examined values were summarized due to the evaluation parameters, mentioned in the **Table 1-II**. For the proper visualization the assumption of the ladle preheating treatment were not included in the following figures. The emission input of this production step was set as 0.29 $kgCO_2/t_{ls}$ during 40 minutes for all the following assumptions. Also this segment, when the ladle is empty, was illustrated partially for the better visualization. Hence, on following **Figure 3-2**, **Figure 3-3** and **Figure 3-4** you can see the CO_2 emission charts under the production step line. These charts also consider the corresponding assumptions: logistic of ladle and lining's configurations.

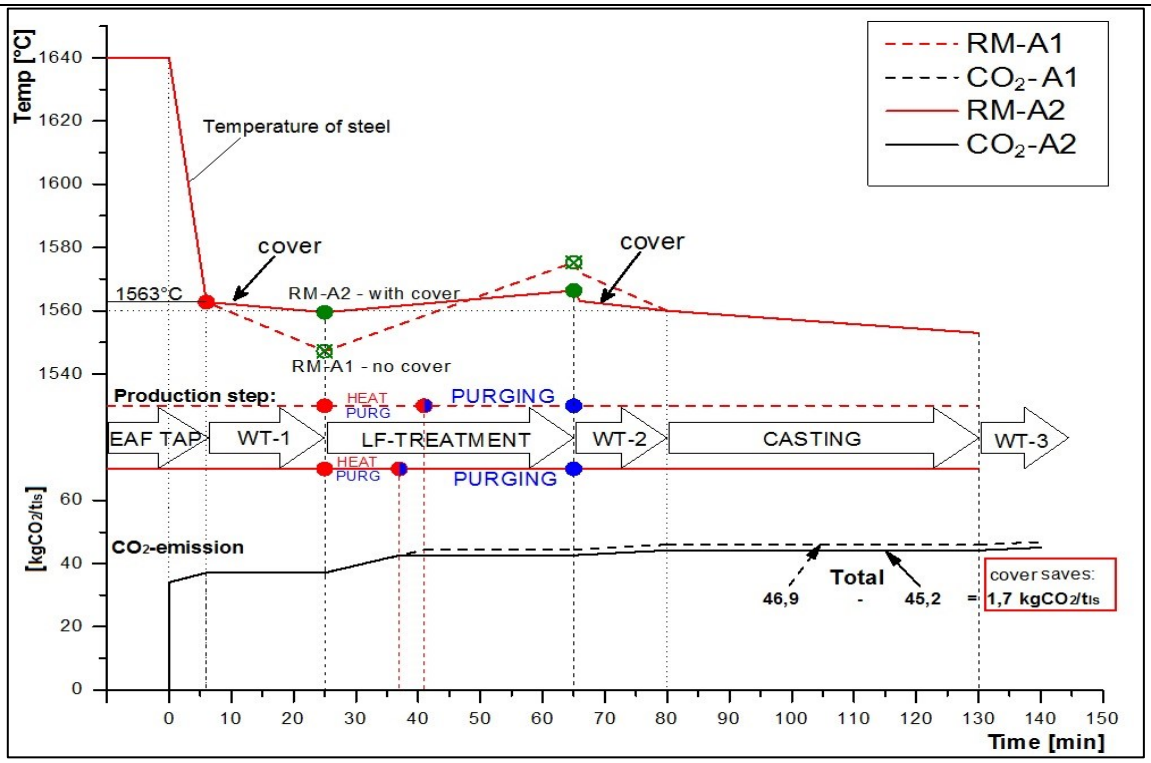

Figure 3-2: Time-temperature charts during one heat for cases "good logistic" RM-A1 (raw magnesite - no cover), RM-A2 (raw magnesite - with cover) due to the production step and related CO_2 emission

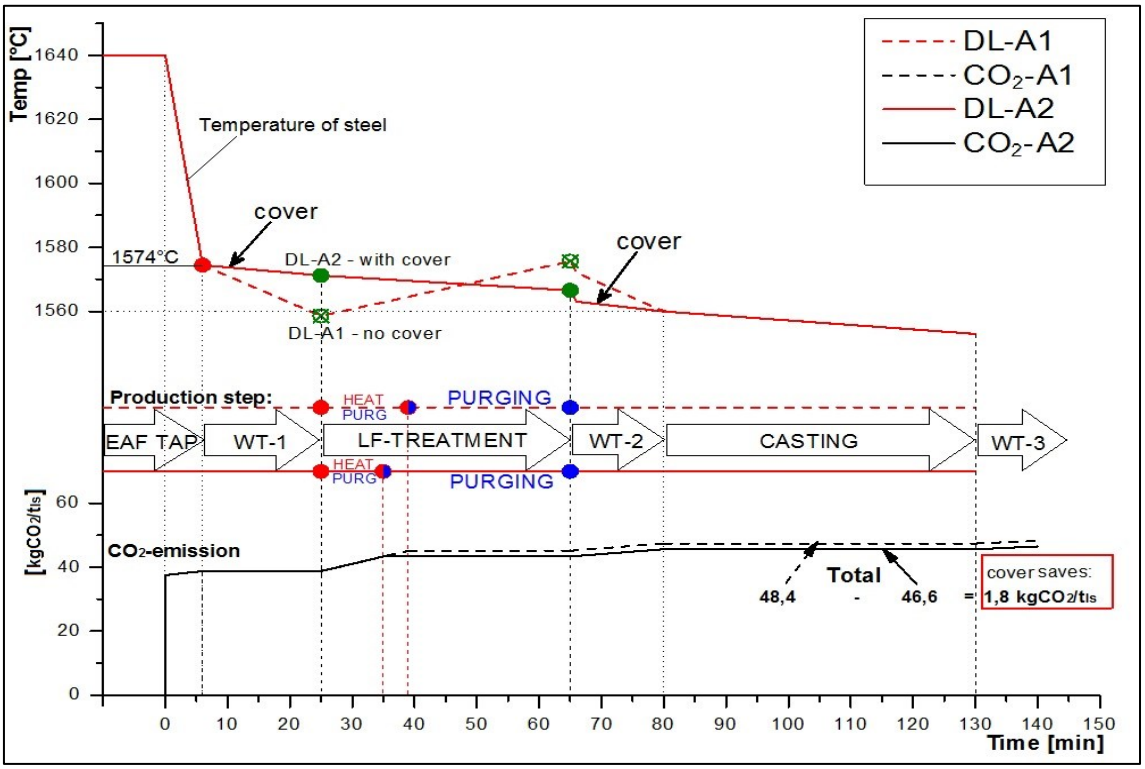

Figure 3-3: Time-temperature charts during one heat for cases "good logistic" DL-A1 (doloma-lime - no cover), DL-A2 (doloma-lime - with cover) due to the production step and related CO_2 emission

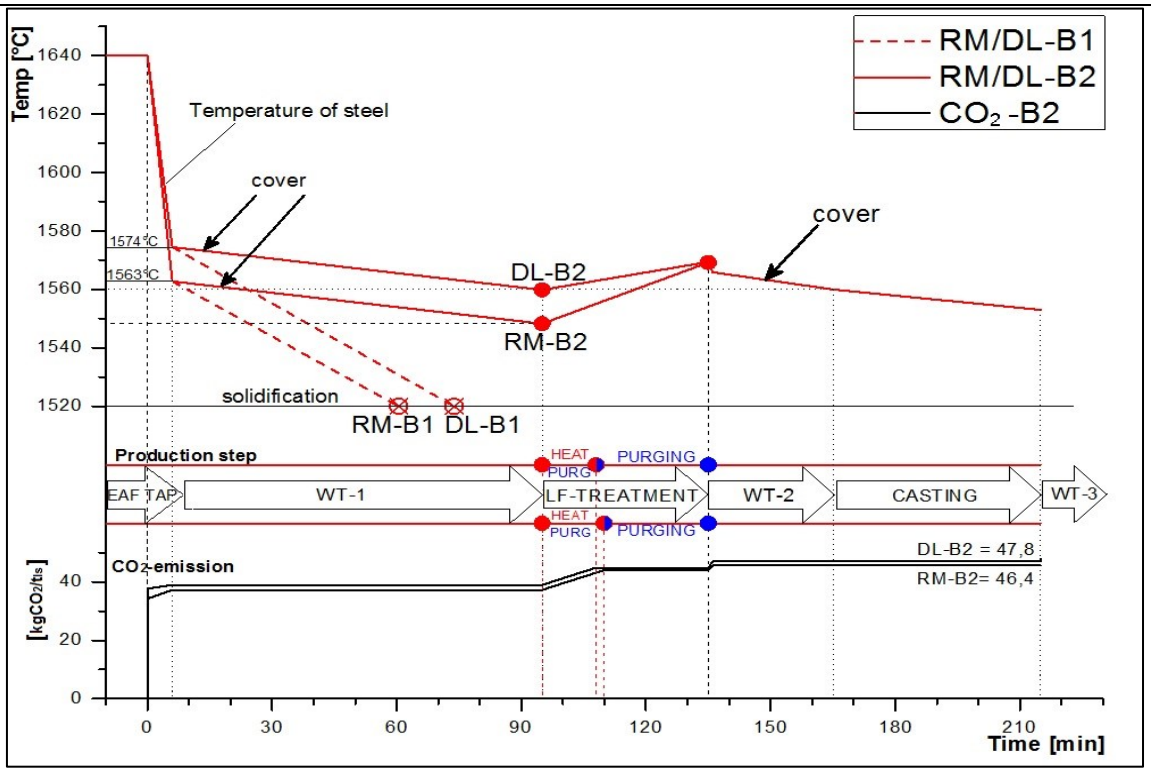

Figure 3-4: Time-temperature charts during one heat for cases “poor logistic” RM-B1 (raw magnesite - no cover), RM-B2 (raw magnesite - with cover), DL-B1 (doloma-lime - no cover) and DL-B2 (doloma-lime - with cover) due to the corresponding production step and related CO_2 emission

4 Conclusions

4.1 Evaluation of the CO_2 savings potential

In the clarification of the task statement of this study, it was assumed to analyse few evaluation items to reduce the CO_2 emissions at the secondary metallurgy (**Table 1-II**).

First, it was decided to compare the variation of alloying concepts using different additions for the slag saturation with MgO – raw magnesite and doloma. Doloma due to its minimal carbon dioxide content seems to be an alternative slag former. The most significant result of this comparison is the potential to reduce the direct emission (*Scope 1*) by alloying more than twice - from 3.06 to 1.27 $kgCO_2/t_{ls}$. Thus, due to the using of different additions for slag saturation it is possible to save 1.79 $kgCO_2/t_{ls}$ of direct emissions, caused by alloying (**Table 2-XV**). Apart from that, alloying mix with usage of doloma is associated with a smaller steel temperature loss caused by alloying - 11°C. Consequently, the smaller temperature loss requires less energy to purchase during the heating by LF-treatment. This reduces the indirect emissions, caused by purchasing of energy (*Scope 2*). But still the alternative alloying concept with using of doloma provides a larger amount of indirect emissions, associated with the purchasing of supply materials (*Scope 3*).

The second item to evaluate was assumed as temperature loss under the consideration of steel contact time. Different temperature losses due to the different logistic and configurations of the ladle imply different energy consumption by LF-treatment, furthermore the different amount of indirect CO_2 emissions, associated with the purchase of electricity. Thus, taking into account the medium emission coefficient - 0.4537 $kgCO_2/kWh$, and the comparison of the corresponding logistic and ladle's configuration assumptions showed, by

means of using a cover it is possible to reduce the emission about 1.68 $kgCO_2/t_{ls}$. Additional logistic improvement of 20% can reduce the emissions from *Scope 2* on 1.10 $kgCO_2/t_{ls}$ (**Table 3-V**). Thus, together these two improvements allow the reduction of the total carbon dioxide input by 2.78 $kgCO_2/t_{ls}$.

Also the prolongation of ladle preheating treatment was evaluated. Taking into account, that preheating is performed only once in 110 heats, then each regular external hour of preheating causes 0.02 $kgCO_2/t_{ls.}$ Thus, the savings potential of reducing the heating treatment duration of 2 hours accounts the saving of 0.04 $kgCO_2/t_{ls}$ (**Table 3-III**).

Thus, to consider the maximal savings potential it was decided to summarize all the estimated sources to reduce the CO_2 emissions at the secondary metallurgy. The potential emission inputs and outputs of each possible improvement are grouped due to the three corresponding *scopes* and included in **Table 4-I**.

Table 4-I: Influence of estimated improvements on the potential savings per tonne of steel

Evaluation item	Improvement	Potential savings per *Scope*, [$kgCO_2/t_{ls}$]			
		1	*2*	*3*	Sum
Additions during tapping for slag saturation with MgO	Substitution of raw magnesite on doloma	+1.83	+0.89	-4.14	-1.42
Configurations of ladle	Usage of ladle cover before and after LF- treatment	-	+1.67	-**	+2.81
Logistic of ladle	Logistic improvement of 85 minutes (~30%)*	-	+1.10	-	
Duration of ladle preheating	Decreasing ladle preheating treatment by 1 hour	+0.04	-	-	
Sum per Scope		+1.87	+3.66	-4.14	+1.39

* - difference between logistic assumptions “poor” and “good” logistic for the corresponding production route.

** - the value does not include the emission, associated with the manufacturing or purchasing of such a ladle cover.

Thus, it is possible to conclude, that substitution of an alloying addition mixusing a doloma will increase the emission input due to the bigger emissions from *Scope 3*. But in fact it is the most significant way to reduce the direct emissions at the secondary metallurgy. The improvement of logistic, as well as the use of a cover during the waiting time segments would reduce the indirect emissions and would increase the energy efficiency. It is important to notice, that the application of a cover is associated with external investments and indirectly would provide emission from *Scope 3*. At the same, time the improvement of logistic requires any investments and implies any other potential emissions.

4.2 Evaluation of the energy-savings potential

The alloying concept with using a doloma (DL-concept) in comparison to the RM-concept is associated with less temperature losses, which in average imply the reduction of energy consumption by LF-treatment by 2 kWh/t_{ls}. Apart from that using a cover and improving of the ladle's logistic also reduces the temperature losses. Evaluation of potential electricity savings was performed by comparison of values, provided in **Table 2-XXVI**. For the common visualization of both influence factors – alloying concept and logistic assumption, it was decided to develop a graph with four scales and three gradients, united through the three dependences in **Figure 4-1**.

First of all, it was assumed to develop a first gradient, which symbolizes the dependence of an addition of raw magnesite (RM) compared with doloma lime (DL) in kg/t_{ls} with total temperature losses per one heat. This principally allows projecting other production capacities with similar chemical requirements. The values differ due to the different amounts of alloying materials required to obtain the same desired MgO saturation. The addition of raw magnesite by current production route is ~4 kg/t_{ls}, addition of doloma is ~4.4 kg/t_{ls}. Each of these concepts was then correlated with the three logistical assumptions. These assumptions are the sum of all estimated temperature losses per heat. Thus, the difference between amounts of temperature to compensate by RM-concept and DL-concept for two identical assumptions A1 (good logistic, no cover) is on average ~8°C.

Next it was decided to connect the amounts of temperature to be compensated during LF-treatment with the amount of required electricity in kWh/t_{ls}. The gradient of 4.23 t_{ls}°C/kWh is based on technical configurations respective to LF and heat size (170 tonnes).

In other words, this gradient shows how many kWh are required to preheat 170 tonnes of steel by 1 °C. The calculation of such gradient was based on the next unit ratio, mentioned in the following equation.

$$y = k \times x \;,\; \left[°C = \frac{°C \times t_{ls}}{kWh} \cdot \frac{kWh}{t_{ls}} \right] \tag{4-1}$$

Thus, specific energy consumption for two identical assumptions A1 by RM-concept is 15.15 and by DL-concept is 13.26 kWh/t_{ls} (**Table 2-XXVI**). Consequently, the specific energy consumption was recalculated to annual energy consumption based on annual steel production 1 Mio tonnes and by corresponding heat size 170 t. By annual steel production of 1 Mio tonnes, 10^6 kWh/t_{ls} are equal to 1 GWh/a. Thus, annual electricity consumption for case of good logistic by RM-concept is 15.14 GWh/a, by DL-concept 13.24 GWh/a.

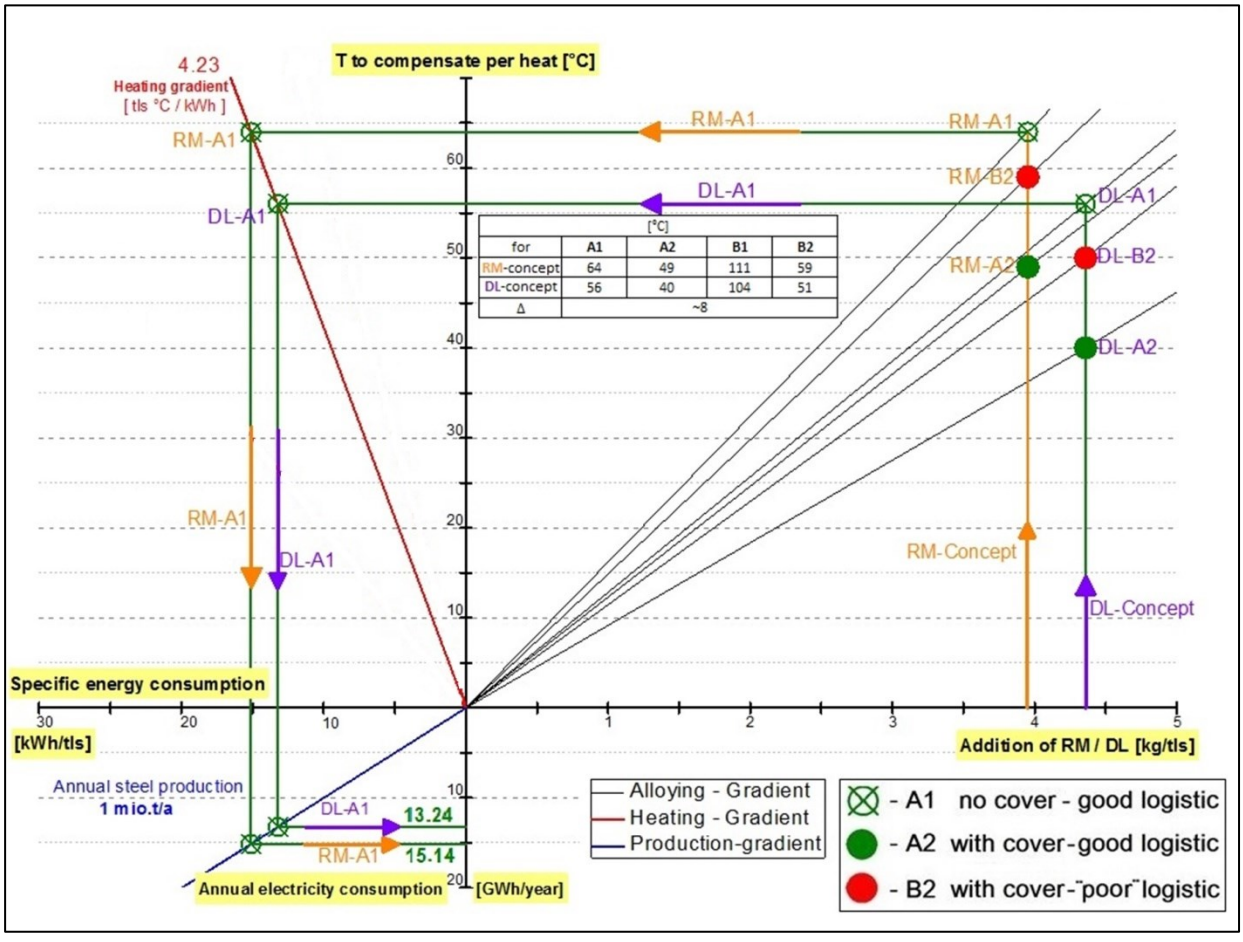

Figure 4-1: Diagram, which compares the alloying concepts and logistic cases RM-A1 (raw magnesite - no cover), RM-A2 (raw magnesite - with cover), DL-A1 (doloma - no cover), DL-A2 (doloma - with cover), RM-B2 (raw magnesite - with cover) and DL-B2 (doloma - with cover) with specific energy consumption and annual electricity consumption

Such chart, like **Figure 4-1**, allows projecting the savings potential values for the production routes with the similar alloying addition mix and LF-configurations. Thus, all the previous calculations can be adopted for any other parameters due to the corresponding requirements.

All estimated annual electricity consumption values for the assumptions mentioned before are included in **Table 4-II**. Also here is shown a comparison of some potential improvements. Hence, in terms of electricity savings, the potential of using a cover during waiting time segments is the most significant improvement. But still, such implementation requires additional financial investments to manufacture or purchase the ladle cover.

Table 4-II: Annual electricity consumption and potential savings by production 1 Mio tones/anno

Assumption	Abb.	RM-concept	DL-concept	Substitution of RM to DL
		[GWh/anno]		
"good" logistic, no cover	A1	15.14	13.24	~1.95
"good" logistic, with cover	A2	11.50	9.52	
"bad" logistic, with cover	B2	13.92	11.96	
Comparison of the assumptions to evaluate the potential electricity savings				
Logistic improvement	B2-A2	2.43		
Using a cover	A1-A2	3.70		

4.3 Potential financial profits

Taking into account the average prices for 1 kWh of electricity - 0.0894 € and 0.34 € per 1 Nm^3 of natural gas, it is possible to recalculate to saving potential to the currency. [58] The calculated values are based on the annual production of 1 million tonnes for corresponding production parameters and included in **Table 4-III**.

Table 4-III: Influence of estimated improvements of the potential annual savings by production 1Mio tonnes steel/a

Improvement	Potential annual savings [€] ,*excluding investments
Substitution of raw magnesite on doloma	170 100*
Using a cover during the delay times	327 600*
Logistic improvement	217 800
Reducing of preheating treatment on 1h	4 500
Sum	**720 000**

References

[1] Dr Brown T., Gratham Institute for Climate Change. Briefing paper No 7: Reducing CO2 emissions from heavy industry: a review of technologies and consideration for policy makers; Available from: https://www.imperial.ac.uk/media/imperial-college/grantham-institute/public/publications/briefing-papers/Reducing-CO2-emissions-from-heavy-industry---Grantham-BP-7.pdf.

[2] United Nations Framework Convention on Climate Change. Kyoto Protocol reference manual: on accounting of emissions and assigned amount; Available from: http://unfccc.int/resource/docs/publications/08_unfccc_kp_ref_manual.pdf.

[3] Brander, M., Ecometrica. Greenhouse Gases, CO2, CO2e and Carbon. What do these terms mean?; Available from: http://ecometrica.com/assets/GHGs-CO2-CO2e-and-Carbon-What-Do-These-Mean-v2.1.pdf.

[4] Intergovernmental Panel on Climate Change (IPCC). IPCC Fourth Assessment Report: Climate Change 2007; Available from: https://www.ipcc.ch/pdf/assessment-report/ar4/wg2/ar4_wg2_full_report.pdf.

[5] Rogner, H.-H., Zhou D., Bradley R., Crabbé P., Edenhofer O., Hare B., Kuijpers L., Yamaguchi M. Contribution of Working Group III to the Fourth Assessment Report of the Intergovernmental Panel on Climate Change, 2007; Available from: http://www.ipcc.ch/pdf/assessment-report/ar4/wg3/ar4-wg3-chapter1.pdf.

[6] Daviet F. Designing a Customized Greenhouse Gas Calculation Tool. World Resources Institute; Available from: http://pdf.wri.org/GHGProtocol-Tools.pdf.

[7] International Energy Agency. Energy technology perspectives 2010; scenarios and strategies to 2050; Available from: https://www.iea.org/publications/freepublications/publication/etp2010.pdf.

[8] Gielen D., Newman J., Patel M.K. Reducing Industrial Energy Use and CO2 Emissions: The Role of Materials Science-MRS BULLETIN Vol.33; Available from: http://journals.cambridge.org/download.php?file=%2FMRS%2FMRS33_04%2FS0883769400005042a.pdf&code=cb17a86821ed5fbeff41ae708a1ef5e1.

[9] Strategic Energy Technologies Information System (SETIS). Energy Efficency and CO2 reduction in the Iron and Steel industry; Available from:

https://setis.ec.europa.eu/system/files/Technology_Information_Sheet_Energy_Efficiency_and_CO2_Reduction_in_the_Iron_and_Steel_Industry.pdf.

[10] J. Schenk and H.B. Lüngen (Montanuniversität Leoben, Leoben, Austria, Steel Institute VDEh, Düsseldorf, Germany). Potentials of direct and smelting reduction processes for an efficient application in Europe 2016;06.2016.

[11] Prof. Schenk J., Dipl. Ing. Buntschuh P., Bsc.Gerasev A. Proof-reading of the article for publication in "RHI-Bulletin" magazine. Montanuniversitaet Leoben, A-8700 Leoben; 2016.

[12] Birat J-P (ed.). The ULCOS program (Ultra Low CO2 Steelmaking); 2015.

[13] The Institute for Industrial Productivity. Ultra-Low CO2 Steelmaking. [May 15, 2016]; Available from: http://ietd.iipnetwork.org/content/ultra-low-co2-steelmaking.

[14] Remus R., Aguado-Monsonet M.A., Roudier S., Sancho L.D. - European Commission, Joint Research Centre, Institute for prospective technological studies. Best Available Techniques (BAT) Reference Document for Iron and Steel Production; Available from: http://eippcb.jrc.ec.europa.eu/reference/BREF/IS_Adopted_03_2012.pdf.

[15] Ghosh A. Secondary Steelmaking: Principles and Applications: CRC Press; 2000.

[16] Stolte G. Secondary metallurgy: Fundamentals, processes, appilcations / Gerd Stolte. Dusseldorf: Verlag Stahleisen; 2002.

[17] Ladle refining [SubsTech]. [August 10, 2016]; Available from: http://www.substech.com/dokuwiki/doku.php?id=ladle_refining.

[18] Dr.-Ing. Helmut Lachmund, AG der Dilliger Hüttenwerke (ed.). "Bedeutung und Aufgaben der Sekundärmetallurgie", Vortrag am Seminar Sekundärmetallurgische Prozesstechnik; 2014.

[19] Hr. Viertauer A., Dr. Trummer B., Dr. Rössler R., Prof. Schenk J., Dipl. Ing. Buntschuh P., Bsc. Gerasev A. Settling of the input-parameters for the developing of alloying concept and calculation basis. Voest Alpine BG04, A-4010 Linz, Austria; 2015.

[20] Hr. Viertauer A., Dr. Trummer B., Dr. Rössler R., Prof. Schenk J., Dipl. Ing. Buntschuh P., Bsc. Gerasev A. Classification of the calculated data, developing of the description diagrams, adaptation of the input-data for the calculation and implementing of the alternative alloying concept. Besprechungszimmer, LfESM, Leoben; 2015.

[21] Hr. Viertauer A., Dr. Trummer B., Dr. Rössler R., Prof. Schenk J., Dipl. Ing. Buntschuh P., Bsc. Gerasev A. Settling of basis for alloying concept and evaluation principle. Voest Alpine Secondary metallurgy department, A-4010 Linz, Austria; 2015.

[22] Wcisło Z., Michalsinzyn A., Baka A., AGH University of Science and Technology, Kraków, Poland. Role of slag in the steel refining process in the ladle 2012;55(2):390–5.

[23] Wuenschendorfer dolomitwerk GmbH. Burnt Dolomite for Metallurgy; Available from: http://dolomitwerk-wuenschendorf.de/fileadmin/user_upload/englisch/Gebr._Dolomit_E_09-11-11.pdf.

[24] Dipl.-Ing. Sebastian Michelic, Ao.Univ.-Prof. Dr. Christian Bernhard. Ferrous Metallurgy II, Module 2 LV-Nr.: 220.042: Eisen- und Stahlmetallurgie II, Mod. 2 – Einführung.

[25] Prof. Schenk J. LV 220.040 - Ferrous Metallurgy I.

[26] Fang X, Yu L, Zhang W, Wang J. Establishment and optimization of prediction model for recovery rate of alloying elements: In: 2012 10th World Congress on Intelligent Control and Automation (WCICA 2012), Beijing, China.

[27] Ao.Univ.-Prof. Dr. Christian Bernhard, Dipl.-Ing. Philip Bundschuh. 220.041 - Lab in ferrous metallurgy-processes, Exicise 2 "LD-Balance": Theoretical calculations in the field of primary and secondary metallurgy; SS 2015.

[28] Prof. Schenk J., Dipl. Ing. Buntschuh P., Bsc. Gerasev A. Settlig of the parameters for the heat balance developing.

[29] Anderson GM, Crerar DA. Thermodynamics in geochemistry: The equilibrium model / Gregor M. Anderson, David A. Crerar. New York: Oxford University Press; 1993.

[30] White'n'white Minerals LTD. Products - Calcined Dolomite; Available from: http://www.burntlime.net/calcined-dolomite.htm.

[31] Satyendra. Lime and calcined dolomite for use in steel plant. [May 19, 2016]; Available from: http://ispatguru.com/lime-and-calcined-dolomite-for-use-in-steel-plant/.

[32] Hobart King. Dolomite: A Mineral and a Rock; Available from: http://geology.com/minerals/dolomite.shtml.

[33] GIMEXCO INTCO. LT. Products profile; Available from: http://www.gimexcomineral.com/.

[34] Dipl.-Ing. Michelic S., Ao.Univ.-Prof. Dr. Bernhard C. Lab in ferrous metallurgy - processes, LV-Nr.: 220.046: Offered in Sommersemester 2013.

[35] Grigoryan V., Stomakhin A., Ponomarenko L., et. al. Physicochemical Calculations of Electric Steelmaking Processes [in Russian]: A Tutorial for Higher Shool.

[36] Buntschuh P. Gerasev A., MUL. Settling of the parameters for heat balance calculation with a using "FactSage"-Software; 2015.

[37] Väyrynen P., Holappa L., Louhenkilpi S., Aalto University, School of Chemical Technology, Espoo, Finland. Simulation of Melting of Alloying Materials in Steel Ladle; Available from: https://www.flow3d.com/wp-content/uploads/2014/08/Simulation-of-Melting-of-Alloying-Materials-in-Steel-Ladle.pdf.

[38] Auerkari P., VTT Manufacturing Technology. Mechanical and physical properties of enginieering alumina ceramics; Available from: http://www.vtt.fi/inf/pdf/tiedotteet/1996/T1792.pdf.

[39] The Engineering ToolBox. Latent Heat of Melting of some common Materials. [May 20, 2016]; Available from: http://www.engineeringtoolbox.com/latent-heat-melting-solids-d_96.html.

[40] Zhang L, Oeters F. Melting and mixing of alloying agents in steel melts: Methods of mathematical modelling. Düsseldorf, Germany: Verlag Stahleisen; 1999.

[41] U.S. Department of Energy FSC-6910. DOE FUNDAMENTALS HANDBOOK THERMODYNAMICS, HEAT TRANSFER, AND FLUID FLOW; Available from: http://www.steamtablesonline.com/pdf/Thermodynamics-Volume2.pdf.

[42] Kabelac S (ed.). VDI-Wärmeatlas: [Berechnungsunterlagen für Druckverlust, Wärme- und Stoffübergang]. Berlin, Heidelberg: Springer-Verlag Berlin Heidelberg; 2006.

[43] Wärmeübertragung: Grundlagen und Praxis. Berlin, Heidelberg: Springer Berlin Heidelberg; 2004.

[44] Buntschuh P. Gerasev A., MUL. Settling of input-parameters for the calculation of heat losses due to the ladle's parameters.

[45] Hr. Viertauer A., Dr. Trummer B., Dr. Rössler R., Prof. Schenk J., Dipl. Ing. Buntschuh P., Bsc. Gerasev A. Clarification of the current calculations. Voest Alpine BG04, A-4010 Linz, Austria; 2016.

[46] Shah RK, Sekulić DP. Fundamentals of heat exchanger design. New York, Chichester: John Wiley & Sons; 2003.

[47] Prof. Schenk J., Bsc. Gerasev A. Settling of concept for calculation of energy consumption of LF-Treatment. Chair of Ferrous Metallurgy, Montanuniversitaet Leoben, A-8700 Leoben; 2015.

[48] Prof. Schenk J., Dipl. Ing. Buntschuh P., Bsc. Gerasev A. Settling the layout calculation vizualization. Chair of Ferrous Metallurgy, Montanuniversitaet Leoben, A-8700 Leoben; 2016.

[49] Grigoriev V., Nechkin Y., Egorov A., Nicolski L. Construction and engineering of steelmaking units (in Russian); 1995.

[50] Prof. Schenk J., Dipl. Ing. Buntschuh P., Bsc. Gerasev A. The settling of emission definition concept for the estimated production route. Chair of Ferrous Metallurgy, Montanuniversitaet Leoben, A-8700 Leoben; 2015.

[51] FlowVision GmbH. Durchflussmessung in Gasen Was ist ein Normkubikmeter? (on german); Available from: http://www.flowvision-gmbh.de/fileadmin/user_upload/FlowVision/pdf-Dateien/Flyer/deutsch/F_Normkubikmeter_1013_d_web.pdf.

[52] Brander M., Sood A., Wylie C., Haughton A., and Lovell J. Electricity-specific emission factors for grid electricity - Technical Paper; Ecometrica; Available from: http://ecometrica.com/assets/Electricity-specific-emission-factors-for-grid-electricity.pdf.

[53] World Steel Association. CO2 EMISSIONS DATA COLLECTION - User Guide, Version 7; Available from: https://www.worldsteel.org/dms/internetDocumentList/downloads/steel-by-topic/Data-collection-user-guide_v6/document/Data%20collection%20user%20guide.pdf.

[54] Lindstad T., Monsen B. and Osen K.S. How the ferroalloys industry can meet greenhouse gas regulations; Available from: http://www.pyrometallurgy.co.za/InfaconXII/063-Lindstad.pdf.

[55] Marks J., Kojo Agyemang-Bonsu W., Firmento Born M., Green L. 2006 IPCC Guidelines for National Greenhouse Gas Inventories, Chapter 4 - Metal industry emissions: 4.4.2.2 CHOICE OF EMISSION FACTORS FOR CO2 EMISSIONS FROM PRIMARY ALUMINIUM PRODUCTION; Available from: http://www.ipcc-nggip.iges.or.jp/public/2006gl/pdf/3_Volume3/V3_4_Ch4_Metal_Industry.pdf.

[56] Ecofys, Fraunhofer Institute for Systems and Innovation Research, Öko-Institut. Sector report for the aluminium industry - Methodology for the free allocation of emission

allowances in the EU ETS post 2012; Available from: http://ec.europa.eu/clima/policies/ets/cap/allocation/docs/bm_study-aluminium_en.pdf.

[57] The European Refractories Producers' Federation (PRE). PRE product carbon footprint report; Available from: http://static1.squarespace.com/static/55b5f359e4b0019200a9482c/t/55b8968be4b08eb536bd5912/1438160523677/PRE+carbon+footprint+methodology+report_final.pdf.

[58] Data from EuroStat website, title „Strompreise nach Art des Benutzers", code: ten00117; Available from: http://ec.europa.eu/eurostat/tgm/table.do?tab=table&plugin=1&language=de&pcode=ten00117.